Dynamic interaction between a moving vehicle and a bridge

Theoretical model and application of a complex mass-spring system, moving across a simply supported bridge

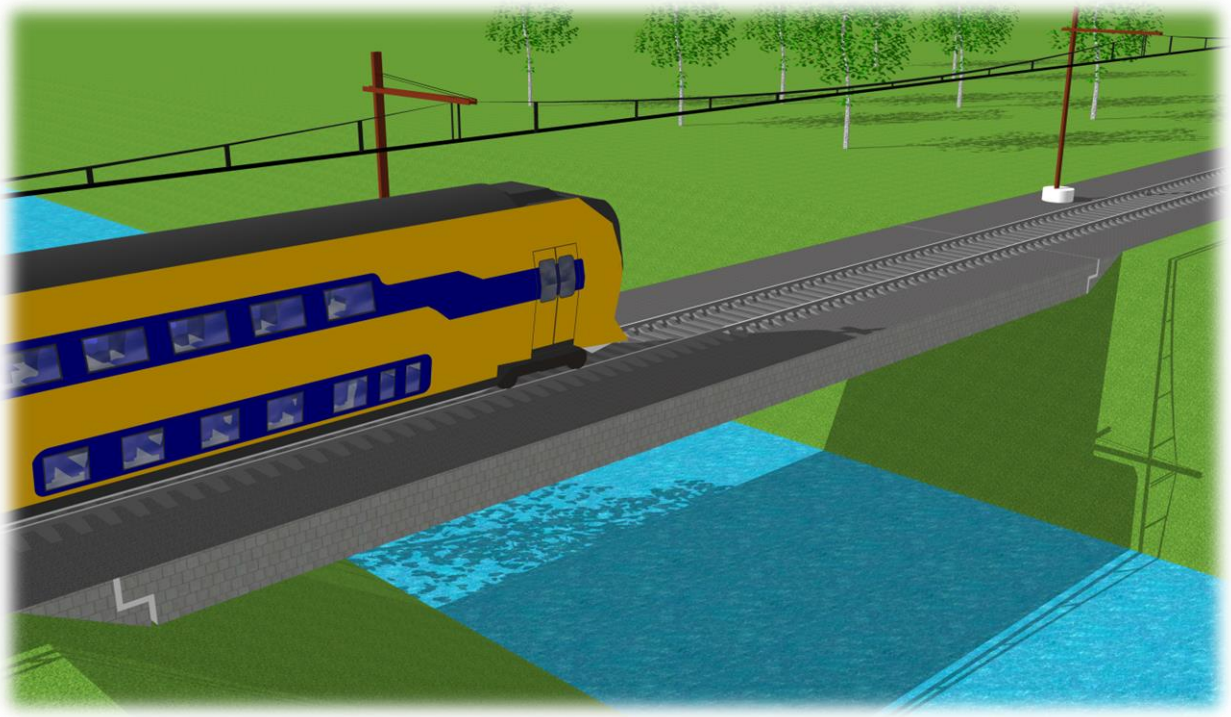

Mark Jol
4536819

Supervisors
dr. ir. Karel van Dalen
ir. Andrei Faragau

TU Delft
17 June 2019

Preface

This thesis was made upon completion of my Bachelor's degree in Civil Engineering at the TU Delft. It involves maths, physics and a lot of programming. If you read this report and have any questions or remarks, feel free to contact me at MarkGCJol at gmail dot com.

Thanks to Karel van Dalen, for providing me with this amazing subject
Thanks to Andrei Faragau, for advising me on the next moves
Thanks to Tim Sluiter, for aiding me wherever possible
Thanks to Cees Smit †, for always believing in me

Summary

When a vehicle moves across a bridge, there is always an interaction between the vehicle and the bridge and within the vehicle itself. It is important to predetermine the vibrations in the bridge and vehicle. This way, the Ultimate Limit State (ULS) and Serviceability Limit State (SLS) can be more accurately determined, compared to a static approach. Ultimate Limit State refers to the safety of the bridge and vehicle. Serviceability Limit State refers to the usability of the bridge and comfort of the passengers. The behaviour of a bridge subjected to a moving load has been researched before. In these studies, the moving vehicle was simplified to a one or two degrees of freedom mass-spring system, which might be insufficient. This thesis aims to investigate the influence of a multiple degrees of freedom oscillator, where the wheels, bogies and wagons are taken into account in the model. The main goal for this thesis is to investigate and describe the vibrations when a vehicle crosses a bridge. More specifically, the importance of the inertia of the vehicle will be assessed for the serviceability limit state (SLS), and ultimate limit state (ULS).

For the vehicle, a passenger train is studied. A train consists of multiple wagons, bogies and wheels, which are all connected with damped springs. To model the train, there are multiple possibilities to reduce the complexity. It is important to start with a relatively simple model and end with an advanced one. The first model consists of a one degree of freedom mass-spring system moving across the bridge with a constant velocity. The second model consists of a two degrees of freedom mass-spring system with rotational inertia. The third model consists of a mass-spring system with six degrees of freedom. All models can consist of one or multiple wagons. For the bridge, the Euler-Bernoulli beam theory is used. This is solved by means of modal expansion. For a moving point load, the equation is solved analytically. For a moving mass-spring system, a numerical approach using the state-space form is applied.

It can be concluded that inertia and the complexity of the vehicle model have a minimal influence on the deflections and moments in the bridge. However, the complexity of the vehicle model has a significant impact on the displacements vertical accelerations of the vehicle itself. However, this is not always the case. Therefore, the influence of the complexity of the vehicle model strongly depends on the properties of the bridge and the velocity of the vehicle. The influence of the velocity on the deflections is large. This is mainly due to resonance of the bridge at critical velocities. At multiple velocities, the different vehicle models show similar results for the deflection of the bridge. When the length of the train is increased to multiple wagons, the results are different compared to a single wagon and resonance peaks can be found at different velocities. The Eurocodes prescribe a static calculation with a dynamic loading factor and disregards the resonance, which is an unsafe approach. According to the findings in this thesis, it might be recommended to prescribe the dynamic calculations in the Eurocodes. In conclusion, neither inertia nor the complexity of the vehicle model have a significant impact on the ultimate limit state and serviceability limit state of the bridge. However, for the ultimate limit state and serviceability limit state of the vehicle the impact is large, since it may lead to lack of comfort or derailment.

Contents

Preface ..... **III**

Summary ..... **IV**

1 Introduction **1**

2 Vehicle model **4**

3 Bridge model **7**

4 Numerical models **9**

4.1 Moving oscillator *9*

4.2 Moving oscillator with rotational inertia *10*

4.3 Moving oscillator with six degrees of freedom *10*

5 Validation of the model **12**

5.1 Numerical solution *12*

5.2 Moving oscillator *13*

5.3 Moving oscillator with rotational inertia *13*

5.4 Moving oscillator with six degrees of freedom *14*

5.5 Required amount of vibration modes *14*

6 Results **16**

6.1 Importance of inertia *16*

6.2 Deflection of the wheels after passing the bridge *20*

6.3 Influence of the velocity *21*

7 Conclusion and recommendations **25**

8 References **26**

Appendix A: Analytical solution **27**

Appendix B: Numerical models in state-space representation **30**

Appendix C: Python code **38**

1 Introduction

When a vehicle moves across a bridge, there is always an interaction between the vehicle and the bridge and within the vehicle itself. This interaction depends on the physical properties of the bridge and the vehicle and can be challenging to model. It is important to predetermine the vibrations in the bridge and vehicle. This way, the Ultimate Limit State (ULS) and Serviceability Limit State (SLS) can be more accurately determined, compared to a static approach. Ultimate Limit State refers to the safety of the bridge and vehicle. Serviceability Limit State refers to the usability of the bridge and comfort of the passengers.
The behaviour of a bridge subjected to a moving load has been researched before. Karl Graff has determined the behaviour of a beam with to a constant moving load. He solved this analytically by means of modal expansion (Graff, 1975). Yang, Yau and Wu have investigated the non-linear dynamic interaction between a beam and a two degrees of freedom mass-spring system, they solved this numerically (Yang, Yau, Wu, 2004). Bilal Ouchene has determined the dynamic interaction of a moving vehicle on a simply supported beam. He compared the results of the point load model with a mass-spring system. The solution was obtained by means of the Green's function approach where the Green's function of the beam was obtained using the modal expansion. (Ouchene, 2017). Anne de Graaf expanded this model with rotational inertia. She used the same numerical method as Ouchene (De Graaf, 2018). In these studies, the moving vehicle was greatly simplified to a one or two degrees of freedom mass-spring system, which might be insufficient. This thesis aims to investigate the influence of a multiple degrees of freedom oscillator, where the wheels, bogies and wagons are taken into account in the model. Also, the solution method differs: the modal expansion method is employed and the resulting set of coupled ordinary differential equations is solved using a time-integration solver.

The main goal for this thesis is to investigate and describe the vibrations when a vehicle crosses a bridge. More specifically, the importance of inertia and complexity of the vehicle model for the serviceability limit state, and ultimate limit state will be assessed.
There are multiple methods to study and model the vibrations of a moving vehicle on a bridge, each of which has their own (dis)advantages. Different options are: Finite element method, Finite Volume Method or modal expansion. For the validation of the model, it is possible to compare to the literature or test this in reality. Finite element method and finite volume method are an option, but they are computationally expensive. On the other hand, modal expansion involves a lot of mathematics and programming, but leads to a fewer amount of degrees of freedom, which can be solved quicker. Therefore, this method is chosen. It is, however, recommended to use different vehicle models to gradually build up complexity. Testing in reality is one of the ways to validate the model. However, this is expensive and time consuming. Due to the limited time span of this thesis, this is not possible. Comparing the results to the literature is also a valuable option. Therefore, the results are compared to the theory of Graff (Graff, 1975).

Chapter 2: Vehicle model will study the physical properties a passenger train, describe the modelling options and present the three applied models.

Chapter 3: Bridge model will give a short description of the Euler-Bernoulli beam theory and its solution. Also, the properties of four common bridges are presented. The analytical derivations of the Euler-Bernoulli beam theory are described in Appendix A.
Chapter 4: Numerical models combines the vehicle and bridge model and describes the equations of motion. A detailed description and the numerical method can be found in Appendix B. The Python code can be found in Appendix C.
Chapter 5: Validation of the model shows that the numerical solution is correct and accurate, and validates the vehicle models with limit cases. Also the number of required vibration modes is determined.
Chapter 6: Results presents a comparison between the models. It describes the importance of inertia and the influence of the velocity.
Chapter 7: Conclusion and recommendations summarises the results and discusses valuable options for further research.

The following symbols and units are used. Note that EI, ρA and vt_i are double letter symbols, which are regarded as one quantity.

Table 1.1: Quantities and units.

Quantity	Symbol	Unit
angle of the vehicle	θ_i	rad
bending stiffness of the bridge	EI	Nm^2
contact force (positive in compression)	Q_i	N
damping	c	Ns/m
Damping ratio of the bridge	ζ	$-$
deflection of the bridge (positive downward)	w	m
displacement of the vehicle (positive downward)	u_i	m
eigenfrequency of the bridge	ω_n	Hz
general transverse loading on the bridge	q	N/m
gravitational acceleration	g	m/s^2
length between the wheels of a wagon	b	m
length of a wagon	s	m
length of the bridge	l	m
mass of the vehicle	m	kg
mass per unit length of the bridge	ρA	kg/m
moment of inertia of the vehicle	J	$kg\ m^2$
position of the front wheel of a wagon	vt_i	m
second moment of area	I	m^4
spring stiffness of the vehicle	k	N/m
time	t	s
vibration mode	n	$-$
Young's modulus	E	N/m^2

Abstract quantities

$$\beta_n = \frac{n\pi}{l},$$

$$\omega_n = \sqrt{\frac{EI}{\rho A}} \left(\frac{n\pi}{l}\right)^2$$

Dirac delta function: $\delta(x - vt)$
Box function: $H(vt) \cdot H(l - vt)$ *

* Note that this is a function of the position of a wheel (vt), usually the time is directly implemented.

2 Vehicle model

For the vehicle, a passenger train is chosen because it may lead to large deflections, induced by the relatively large mass and the amount of springs and dampers. Also, in recent years, cracks and other types of deterioration have been observed in train bridges. In order to understand the importance of inertia, multiple models are made to gradually build up complexity. This way, the results can be compared.
To model a train, it is important to have a good idea of the different elements and how these can be implemented, so that the models can be justified. Therefore, this chapter gives a detailed picture and the physical properties of a passenger train, shows different modelling options, determines the relevant ones and elaborates mathematically on three suitable train models.

First of all, an analysis of the vehicle is made. A passenger train consists of multiple wagons, bogies and wheels. Figure 2.1 shows that every wagon is carried by two bogies, each are supported by four wheels. Figures 2.2 and 2.3 take a closer look at two different bogies and show that the connection with the wagon and wheels contains springs and dampers. Furthermore, it becomes visible that there is a direct steel-on-steel contact between the rails and the wheels. Table 2.1 presents the relevant properties of a passenger train.

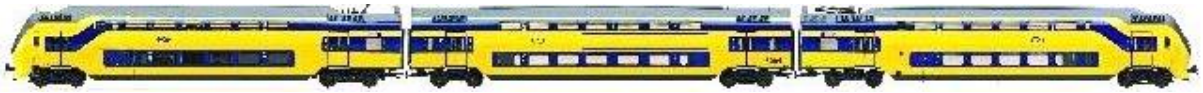

Figure 2.1: side view of a train (Tee USA, 2007)

Figure 2.2: bogie of a train (Wikipedia, 2018)

Figure 2.3: alternative bogie (Wikipedia, 2018)

Table 2.1: Train properties (Canetta, 2017)

Quantity	Symbol	Value	Unit
length of a wagon	s	24.9	m
distance between the wheels	b	17.4	m
velocity	v	50 - 100	m/s
mass of a wagon	m_1	$15.6 \cdot 10^3$	kg
mass of a bogie	m_2	$3.2 \cdot 10^3$	kg
mass of a wheel	m_3	$1.5 \cdot 10^3$	kg
stiffness wagon-bogie	k_1	$1.2 \cdot 10^6$	N/m
stiffness bogie-wheel	k_2	$4.4 \cdot 10^6$	N/m
stiffness wheel-rails	k_3	$1.27 \cdot 10^9$	N/m
damping wagon-bogie	c_1	$34.44 \cdot 10^3$	Ns/m
damping bogie-wheel	c_2	$52.21 \cdot 10^3$	Ns/m

Secondly, the modelling options are further examined. To model the train, there are multiple possibilities to reduce the complexity: there is the possibility to model a single wagon or multiple wagons; a wagon (or two half wagons) can be modelled to have a single bogie, or a wagon can be modelled to have two bogies with the rotational inertia of the wagon itself; a bogie can be modelled with a two wheels or four wheels, where rotational inertia of the bogie is taken into account. The connections between the different elements can be modelled as a direct (stiff) connection or with springs and dampers. Since the wheels could come lose from the rails, its connection can be modelled as a bilinear spring, so that only a compressive force can be applied. The rotational inertia of the bogies is difficult to model and the distance between the wheels is relatively short. Therefore, the bogies will be modelled with a set of two wheels on the same place. Apart from that, every complexing step that is mentioned here, is utilized.

It is important to start with a relatively simple model and end with an advanced model. This way, every model can be verified with the previous one and shows the influence of the added degree of freedom. This thesis elaborates on three models: a one degree of freedom moving oscillator, a two degrees of freedom moving oscillator with rotational inertia and a moving oscillator with six degrees of freedom. All three are mathematically described.

Moving oscillator

The first model consists of one or more mass-spring systems moving across the bridge with a constant velocity. Since this model is a simplification, the parameters are adapted. Every mass consists of half the mass of a wagon. The connection with the beam is modelled with a single spring and damper. The calculations of the spring stiffness and damping constant are shown in equation 2.1. Figure 2.4 gives a graphical representation of the moving oscillator.

$$\begin{aligned} m &= \frac{m_1}{2} + m_2 + 4m_3 \\ k &= \left(\frac{1}{k_1} + \frac{1}{4k_2} + \frac{1}{4k_3}\right)^{-1} \\ c &= \left(\frac{1}{c_1} + \frac{1}{4c_2}\right)^{-1} \end{aligned} \tag{2.1}$$

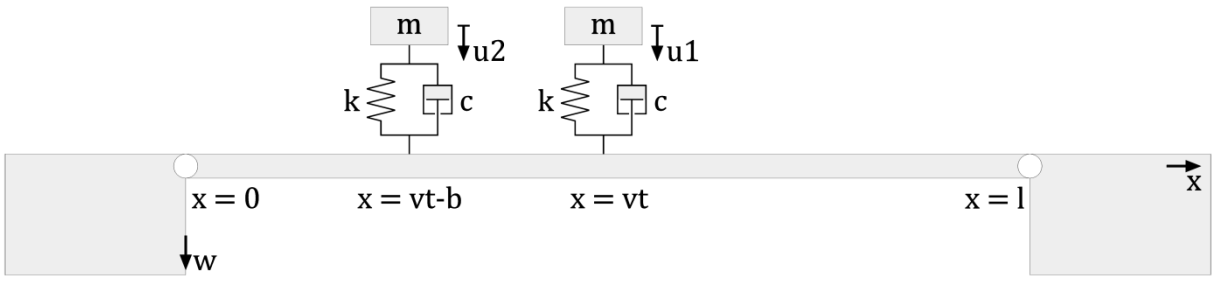

Figure 2.4: Moving oscillator

Moving oscillator with rotational inertia

The second model consists of one or more mass-spring systems with rotational inertia moving across the bridge with a constant velocity. Since this model is also a simplification, the parameters are adapted. Every mass consists of the total mass of a wagon. The connection with the beam is modelled with a two springs and dampers,

which have the same properties as in the previous model. The calculations of the mass and rotational inertia are shown in equation 2.2. Figure 2.5 gives a graphical representation of the moving oscillator with rotational inertia.

$$m = m_1 + 2m_2 + 8m_3$$
$$J = \frac{1}{12} m_1 s^2 + (2m_2 + 8m_3)\left(\frac{b}{2}\right)^2 \tag{2.2}$$

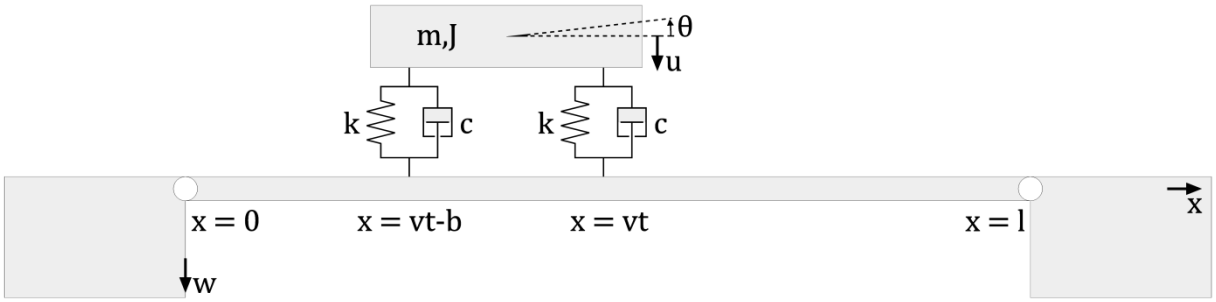

Figure 2.5: Moving oscillator with rotational inertia

Moving oscillator with six degrees of freedom

The third model consists of one or more mass-spring systems with six degrees of freedom moving across the bridge with a constant velocity. This model describes the reality rather accurately: masses, spring stiffness's and damping constants can be directly implemented. The connections within the train itself are modelled with springs and dampers. The connection between the train and the bridge is modelled with a bilinear spring, which only applies a force in compression. This way, the wheels can lift from the rails. Equation 2.3 presents the value for the rotational inertia, which differs from the previous model. Figure 2.6 gives a graphical representation of the moving oscillator with six degrees of freedom.

$$J = \frac{1}{12} m_1 s^2 \tag{2.3}$$

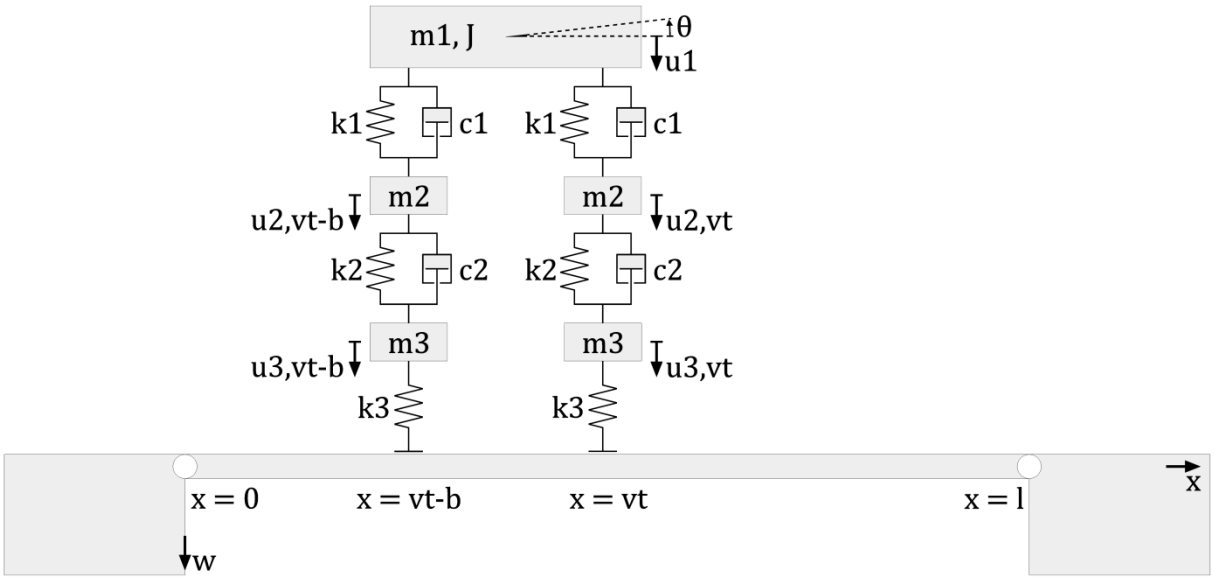

Figure 2.6: Moving oscillator with six degrees of freedom

3 Bridge model

For the bridge model, either the Euler-Bernoulli or Timoshenko beam theory can be used. To make a comparison: the Euler-Bernoulli is derived from the linear theory of elasticity; it is used to calculate the stresses and deflection of a beam. This theory is suitable in case of lateral loads and small deflections (Ravetz, 1962). Timoshenko, on the other hand, also takes into account shear deformation and torsion. This makes it suitable for describing relatively thick beams with bigger deflections or wavelengths that approach the thickness of the beam (Timoshenko, 1932). Since the relatively thin beam in this thesis contains only lateral loads, contains small deflections and is not subjected to rotational bending, the Euler-Bernoulli beam theory is a logical choice. Therefore, this method is further elaborated.

The bridge is assumed to be a simply supported beam, the bridgeheads are assumed to be rigid. The load is defined as the sum of multiple point loads, moving across the bridge with a constant velocity. These are further specified in chapter 4. For the simply supported bridge, the deflections and moments are zero at the supports, which means that the boundary conditions are zero. The intrinsic weight of the bridge is generally taken into account during the construction of the bridge, which means that the bridge is flat at completion. This means the initial conditions are zero as well. These assumptions lead to the following set of equations.

$$EI\frac{\partial^4 w}{\partial x^4}(x,t) + c_d I\frac{\partial^5 w}{\partial x^4 \partial t}(x,t) + \rho A\frac{\partial^2 w}{\partial t^2}(x,t) = q(x,t) \tag{3.1}$$

$$q(x,t) = \sum_i Q_i(t)\cdot\delta(x - vt_i)\cdot H(vt_i)\cdot H(l - vt_i)$$
$$vt_i = v\cdot t - s_i - b_i \tag{3.2}$$

$$\begin{aligned} w(0,t) &= 0 \qquad & \frac{\partial^2 w}{\partial x^2}(0,t) &= 0 \\ w(l,t) &= 0 \qquad & \frac{\partial^2 w}{\partial x^2}(l,t) &= 0 \\ w(x,0) &= 0 \qquad & \frac{\partial w}{\partial t}(x,0) &= 0 \end{aligned} \tag{3.3}$$

The Euler-Bernoulli beam equation is solved by means of modal expansion. For each vibration mode, the x-dependant part of the deflection is determined analytically. A step-by-step derivation of this can be found in appendix A. The time dependant part of the deflection cannot (yet) be solved analytically for a moving mass-spring system. Therefore, this is done numerically. Appendices B and C elaborate further on this. The total solution is the multiplication of the time dependant and x-dependant part of the deflection of the beam, summed for each mode. This is shown mathematically in the following equations.

$$w(x,t) = \sum_{n=1}^{\infty} w_{xn}(x) \cdot w_{tn}(t) \tag{3.4}$$

$$w_{xn}(x) = \sin(\beta_n x) \tag{3.5}$$

$$\begin{gathered} \frac{\partial^2 w_{tn}}{\partial t^2}(t) + 2\zeta\omega_n \frac{\partial w_{tn}}{\partial t}(t) + {\omega_n}^2 w_{tn}(t) = \sum_i f_n(vt_i) \cdot Q_i(t) \\ f_n(vt) = \frac{2\ \sin(\beta_n vt)}{\rho A l} \cdot H(vt) \cdot H(l - vt) \\ \zeta = \frac{c_d I}{2\sqrt{EI\ \rho A}} \left(\frac{n\pi}{l}\right)^2 \end{gathered} \tag{3.6}$$

Equation 3.7 presents the analytical solution to this differential equation (Graff, 1975). The solution only holds when Q_i is on the bridge and consist of a single moving point load, not influenced by the bridge. Also the damping is not taken into account.

$$w(x,t) = \frac{2Q}{\rho A l} \sum_{n=1}^{\infty} \frac{\sin(\beta_n x)}{\omega_n\left({\beta_n}^2 v^2 - {\omega_n}^2\right)} \left(\beta_n v \sin(\omega_n\, t) - \omega_n \sin(\beta_n\, vt)\right) \tag{3.7}$$

There are many different bridges, all with varying properties. In order to study the importance of inertia and obtain a complete picture, four bridges are selected. These are varying in length and are representable for commonly constructed bridges. Table 3.1 shows the characteristics of these bridges (Arvidsson, Karoumi, Pacoste, 2013).

Table 3.1: Bridge properties

Quantity	Bridge 1	Bridge 2	Bridge 3	Bridge 4	Unit	
l	6	12	24	36		m
EI	3.33	12.55	53.38	172.2	$\cdot 10^9$	Nm^2
ρA	8.83	12.3	19.3	17.0	$\cdot 10^3$	kg/m
ζ	2.48	2.06	1.50	0.50		%

4 Numerical models

Introduction

It is important to make multiple models to gradually build up complexity, this way the results can be compared. Therefore, this chapter covers three different models of the vehicle: a one degree of freedom moving oscillator, a two degrees of freedom moving oscillator with rotational inertia, and a moving oscillator with six degrees of freedom. The analytical solution for a moving mass-spring system interacting with a simply supported bridge is (yet) unknown. Therefore, the solution is obtained numerically, this is done by rewriting the equations in state-space form. A detailed description of the numerical models is covered in Appendix B. The Python code is presented in Appendix C. To calculate the moment distribution in the bridge and the vertical accelerations of the train, the second derivative of the deflection to x, respectively to time are needed. Therefore, spline interpolation is applied. This way, the results are more accurate, compared to other numerical methods. A side note should be added that for the relative vertical velocity of the vehicle and the bridge, there is not accounted for the influence of the horizontal velocity of the vehicle (equation 4.2, 4.5 and 4.8).

4.1 Moving oscillator

The first model consists of one or more mass-spring systems moving across the bridge with a constant velocity. Every oscillator represents half a wagon, where the rotational inertia is disregarded, and the connections are simplified to a single spring and damper. The mass of the vehicle is subjected to gravity and the contact force with the bridge. This contact force depends on the relative displacement and vertical velocity of the vehicle, compared to the bridge. The vehicle is assumed to be in the steady state position when entering the bridge. This leads to the following set of equations and graphical representation.

$$m\ddot{u}_i(t) = mg - Q_i(t) \tag{4.1}$$

$$\begin{aligned} Q_{i,1}(t) &= k\left(u_{i,1}(t) - w(vt_i, t)\right) + c\left(\dot{u}_{i,1}(t) - \dot{w}(vt_i, t)\right) \\ Q_{i,2}(t) &= k\left(u_{i,2}(t) - w(vt_i - b, t)\right) + c\left(\dot{u}_{i,2}(t) - \dot{w}(vt_i - b, t)\right) \end{aligned} \tag{4.2}$$

$$u_i(0) = \frac{mg}{k} \qquad \dot{u}_i(0) = 0 \tag{4.3}$$

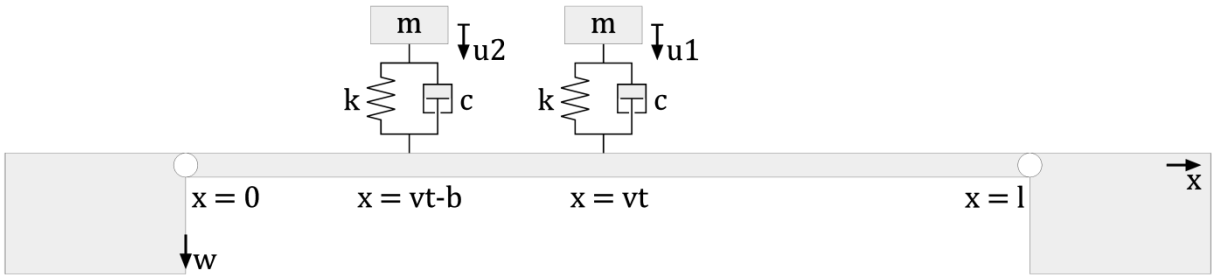

Figure 4.1: Moving oscillator

4.2 Moving oscillator with rotational inertia

The second model consists of one or more mass-spring systems with rotational inertia moving across the bridge with a constant velocity. Every moving oscillator represents a wagon, where the rotational inertia is taken into account and the connections are simplified to a single spring and damper. This leads to the following set of equations and graphical representation.

$$\begin{aligned} m\ddot{u}_i(t) &= mg - Q_{i,vt}(t) - Q_{i,vt-b}(t) \\ J\ddot{\theta}_i(t) &= \frac{b}{2}\left(Q_{i,vt}(t) - Q_{i,vt-b}(t)\right) \end{aligned} \tag{4.4}$$

$$\begin{aligned} Q_{i,vt}(t) &= \left(u_i(t) - \frac{1}{2}b\,\theta_i(t) - w(vt_i,t)\right) + c\left(\dot{u}_i(t) - \frac{1}{2}b\,\dot{\theta}_i(t) - \dot{w}(vt_i,t)\right) \\ Q_{i,vt-b}(t) &= k\left(u_i(t) + \frac{1}{2}b\,\theta_i(t) - w(vt_i - b,t)\right) + c\left(\dot{u}_i(t) + \frac{1}{2}b\,\dot{\theta}_i(t) - \dot{w}(vt_i - b,t)\right) \end{aligned} \tag{4.5}$$

$$\begin{aligned} u_i(0) &= \frac{mg}{2k} & \dot{u}_i(0) &= 0 \\ \theta_i(0) &= 0 & \dot{\theta}_i(0) &= 0 \end{aligned} \tag{4.6}$$

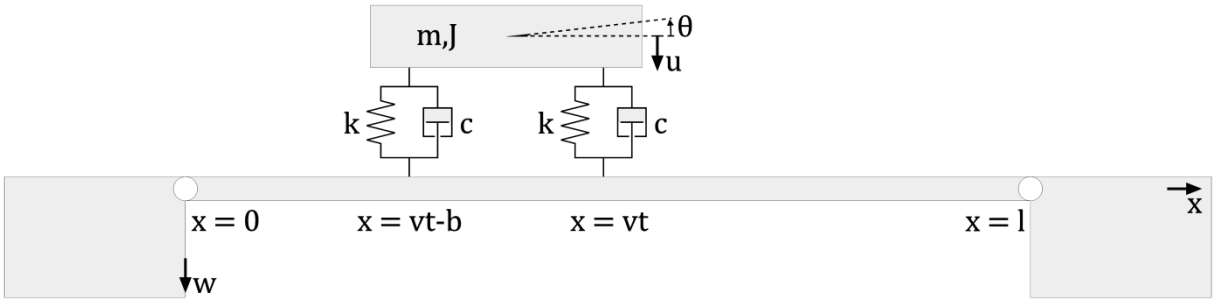

Figure 4.2: Moving oscillator with rotational inertia

4.3 Moving oscillator with six degrees of freedom

The third model consists of one or more mass-spring systems with six degrees of freedom moving across the bridge with a constant velocity. Every moving oscillator represents a wagon, where the rotational inertia, mass of the bogies and wheels are taken into account. The mass of the wagon is subjected to gravity and the contact force with the bogies. The wheels are also subjected to the contact force with the bridge, which is only applied in compression. The contact forces consist of the relative displacement and vertical velocity of the relevant parts. All parts of the vehicle are assumed to be in the steady state position when entering the bridge. This leads to the set of equations and graphical representation on the next page.

$$
\begin{aligned}
m_1\ddot{u}_{i1}(t) &= m_1 g - Q_{i1,vt}(t) - Q_{i1,vt-b}(t) \\
J\ddot{\theta}_i(t) &= \frac{b}{2}\left(Q_{i1,vt}(t) - Q_{i1,vt-b}(t)\right)
\end{aligned}
$$

$$
\begin{aligned}
m_2\ddot{u}_{i2,vt}(t) &= m_2 g + Q_{i1,vt}(t) - Q_{i2,vt}(t) \\
m_2\ddot{u}_{i2,vt-b}(t) &= m_2 g + Q_{i1,vt-b}(t) - Q_{i2,vt-b}(t)
\end{aligned}
\tag{4.7}
$$

$$
\begin{aligned}
m_3\ddot{u}_{i3,vt}(t) &= m_3 g + Q_{i2,vt}(t) - Q_{i3,vt}(t) \\
m_3\ddot{u}_{i3,vt-b}(t) &= m_3 g + Q_{i2,vt-b}(t) - Q_{i3,vt-b}(t)
\end{aligned}
$$

$$
\begin{aligned}
Q_{i,1,vt}(t) &= k_1\left(u_{i,1}(t) - \frac{1}{2}b\,\theta_i(t) - u_{i,2,vt}\right) + c_1\left(\dot{u}_{i,1}(t) - \frac{1}{2}b\,\dot{\theta}_i(t) - \dot{u}_{i,2,vt}\right) \\
Q_{i,1,vt-b}(t) &= k_1\left(u_{i,1}(t) + \frac{1}{2}b\,\theta_i(t) - u_{i,2,vt-b}\right) + c_1\left(\dot{u}_{i,1}(t) + \frac{1}{2}b\,\dot{\theta}_i(t) - \dot{u}_{i,2,vt-b}\right)
\end{aligned}
$$

$$
\begin{aligned}
Q_{i,2,vt} &= k_2\left(u_{i,2,vt} - u_{i,3,vt}\right) + c_2\left(\dot{u}_{i,2,vt} - \dot{u}_{i,3,vt}\right) \\
Q_{i,2,vt-b} &= k_2\left(u_{i,2,vt-b} - u_{i,3,vt-b}\right) + c_2\left(\dot{u}_{i,2,vt-b} - \dot{u}_{i,3,vt-b}\right)
\end{aligned}
\tag{4.8}
$$

$$
\begin{aligned}
Q_{i,3,vt} &= k_3\left(u_{i,3,vt}(t) - w(vt_i, t)\right) \cdot H\left(u_{i,3,vt}(t) - w(vt_i, t)\right) \\
Q_{i,3,vt-b} &= k_3\left(u_{i,3,vt-b}(t) - w(vt_i - b, t)\right) \cdot H\left(u_{i,3,vt-b}(t) - w(vt_i - b, t)\right)
\end{aligned}
$$

$$
\begin{aligned}
u_{i,1}(0) &= u_{i,2}(0) + \frac{m_1}{2k_1}g & \dot{u}_{i,1}(0) &= 0 \\
\theta_i(0) &= 0 & \dot{\theta}_i(0) &= 0 \\
u_{i,2}(0) &= u_{i,3}(0) + \frac{m_1 + 2m_2}{2k_2}g & \dot{u}_{i,2}(0) &= 0 \\
u_{i,3}(0) &= \frac{m_1 + 2m_2 + 2m_3}{2k_3}g & \dot{u}_{i,3}(0) &= 0
\end{aligned}
\tag{4.9}
$$

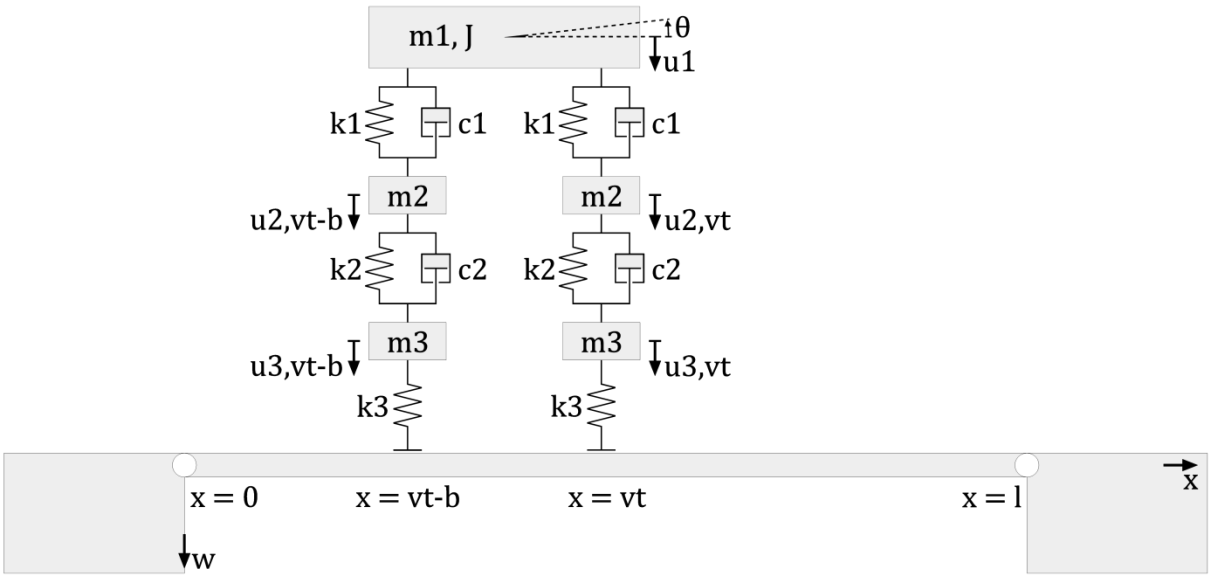

Figure 4.3: Moving oscillator with six degrees of freedom

5 Validation of the model

Introduction

In order to present reliable results, it is important to compare these to the literature. In this case, the numerical model is compared to Graff's solution (Graff, 1975). Then the more advanced models are validated by considering limit cases against each other. The moving oscillator is compared to point loads considering the limit case $m \to 0$ to see if the extra degree of freedom for the vehicle is well implemented. Then the moving oscillator with rotational inertia is compared to the moving oscillator considering the limit case $b = 0$ to see if the rotational inertia is well implemented. Finally, the moving oscillator with six degrees of freedom is tested against the moving oscillator with rotational inertia considering the limit case $m_2 = m_3 \to 0$ to see if the extra degrees of freedom are well implemented. Equation 5.1 defines the relative error, where the sum of the errors over time are calculated. All figures in this chapter show a comparison between two methods, with the bridge response on the left and the relative errors on the right. Comparisons are made utilizing bridge 4, considering 10 vibration modes.

$$e = \frac{\sum_t |w(x,t) - w_{ref}(x,t)|}{\sum_t |w_{ref}(x,t)|} \tag{5.1}$$

5.1 Numerical solution

The numerical solution is checked against the solution presented by Graff (equation 3.7) (Graff, 1975). This is done with a single moving point load (equations B.1-B.4). Figure 5.1 shows the deflection of the bridge and the error over the length of the bridge. This results in an average relative error of $3.3 \cdot 10^{-9}$, which means that the model is precise.

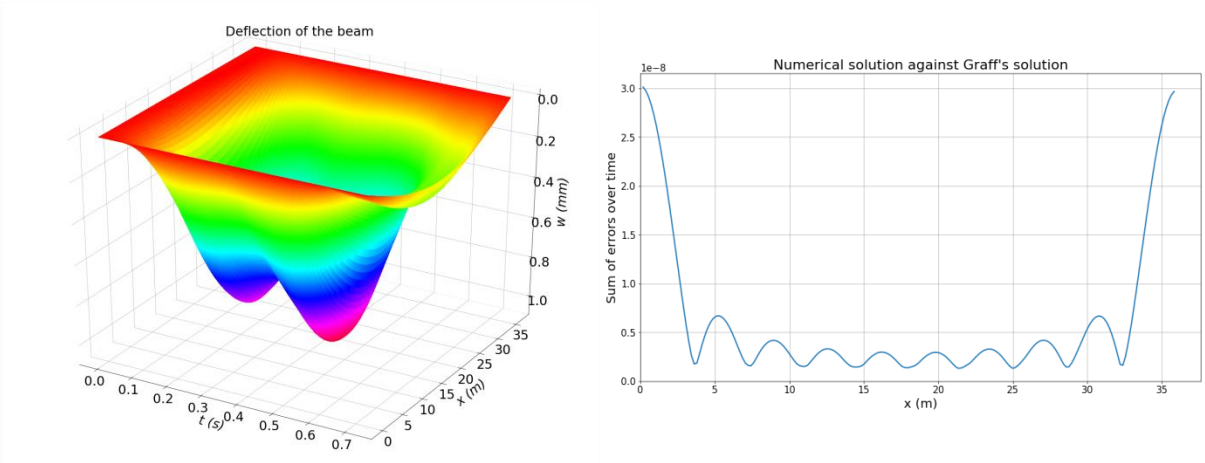

Figure 5.1: Numerical against analytical solution

5.2 Moving oscillator

The moving oscillator is then compared to the moving point load model by considering the limit case $m \to 0$. This is done by modelling a single moving point load, where the gravitation of the low mass is compensated with an external force. Figure 5.2 shows the deflection of the bridge and relative error over the length of the bridge. This results in an average relative error of $2.4 \cdot 10^{-6}$. This means that the extra degree of freedom for the vehicle is well implemented.

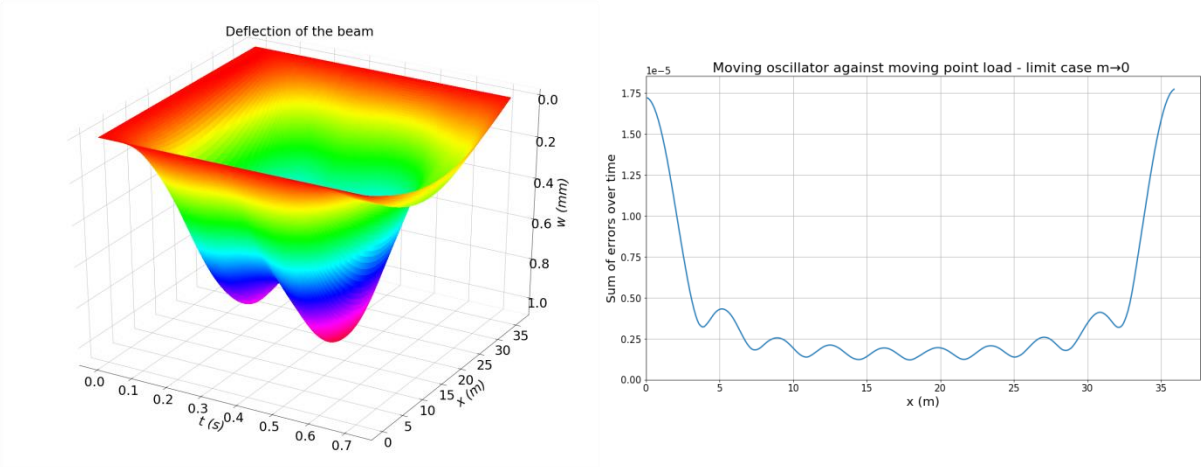

Figure 5.2: The moving oscillator compared to the moving point loads considering the limit case $m \to 0$

5.3 Moving oscillator with rotational inertia

The moving oscillator with rotational inertia is compared to the moving oscillator by considering the limit case $b = 0$. Figure 5.3 shows the deflection of the bridge and relative error over the length of the bridge. This results in the sum of all errors of $2.3 \cdot 10^{-4}$, which can be explained by a numerical error. This means that the extra degree of freedom is well implemented.

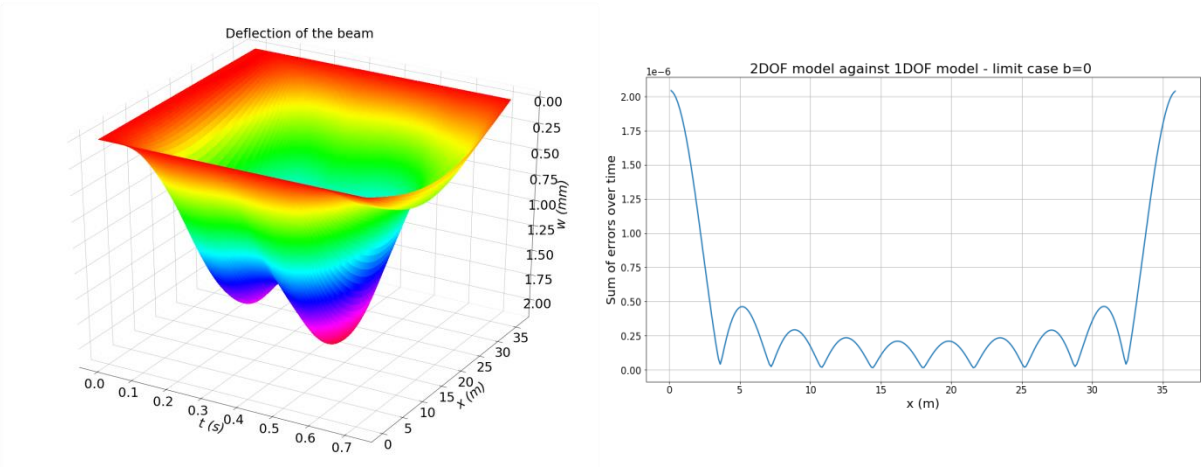

Figure 5.3: Moving oscillator with rotational inertia compared to the moving oscillator considering the limit case $b = 0$

5.4 Moving oscillator with six degrees of freedom

The moving oscillator with six degrees of freedom is compared to the moving oscillator with rotational inertia by considering the limit case $m_2 = m_3 = 0$. The difference in mass and rotational inertia is accounted for in the model. Figure 5.4 shows the deflection of the bridge and relative error over the length of the bridge. This results in an average relative error of $1.4 \cdot 10^{-5}$. This means that the extra degrees of freedom are well implemented.

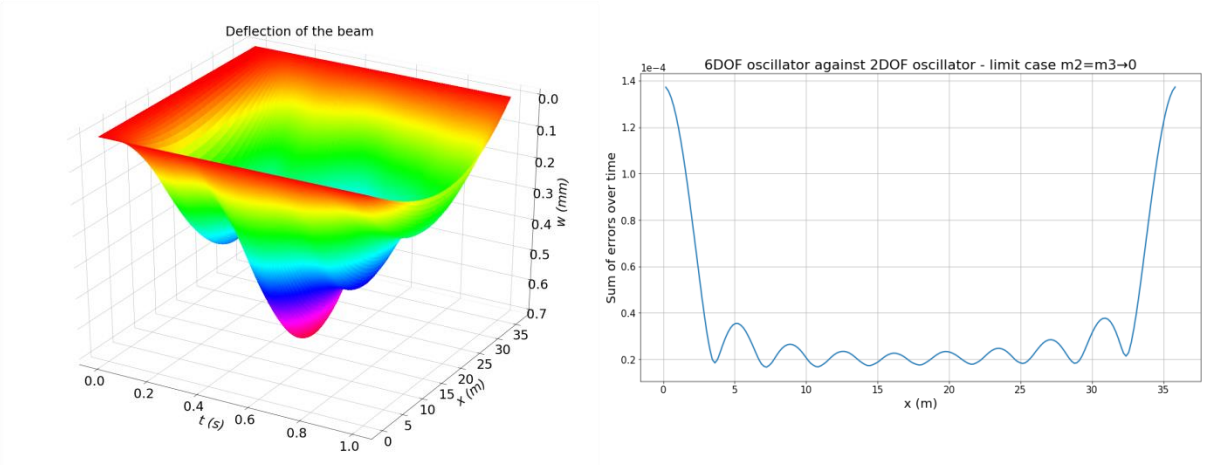

Figure 5.4: Moving oscillator with six degrees of freedom compared to moving oscillator with rotational inertia considering the limit case $m_2 = m_3 = 0$

5.5 Required amount of vibration modes

Since the solution consist of an infinite amount of vibration modes, there needs to be determined how many vibration modes are required for a reliable result. In order to do so, results of the deflection are obtained with multiple vibration modes, starting with one vibration mode and building up to fifty. The deflections of the bridge are compared to the deflections with fifty vibration modes. The results are shown in figure 5.5 on the next page.

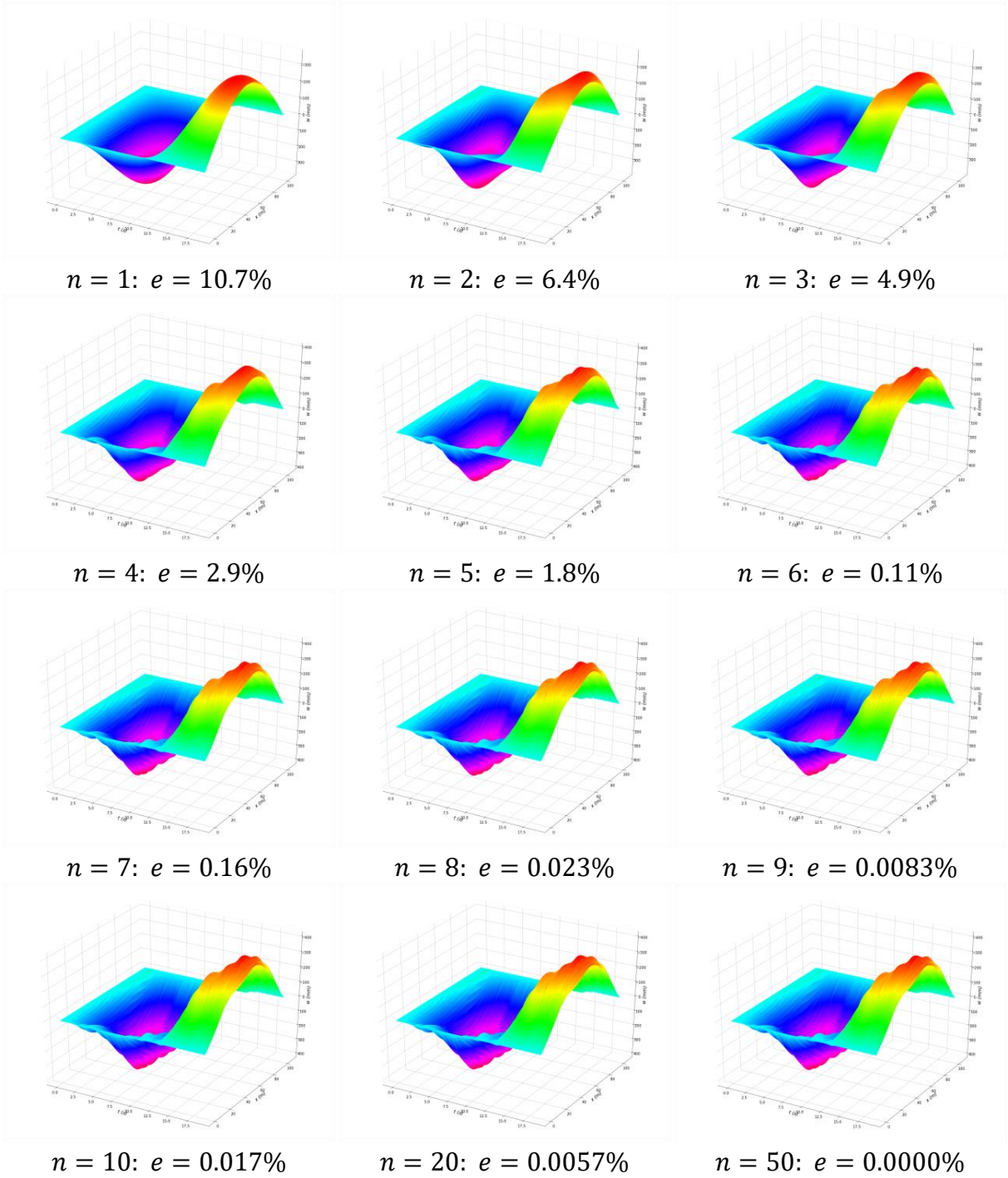

Figure 5.5: Influence of the amount of vibration modes on the error, compared to $n = 50$

It is fair to say that in all cases, descent results are obtained. However, an n-value of 6 or greater is advised for a reliable result. In this thesis, a value of 10 is chosen. It is worth noting that when the values for the bending moments and vertical accelerations are compared. More nodes are required to get accurate results. This in turn leads to an increase of the computation time. Therefore, a bigger error is accepted for the bending moments and vertical accelerations.

6 Results

Introduction

In this chapter, results, visual representations of the deflections and interpretations are presented. Firstly, a comparison is made between the different models regarding ULS and SLS, where ULS refers to the bending moments in the bridge and deflections of the wheels and SLS refers to the deflections of the bridge and vertical accelerations of the vehicle. Then, it is investigated whether the wheels lose contact with the rails, which is important since it may lead to fatigue or derailment. Finally, the influence of the velocity on the maximum deflection is assessed; this is done by studying 1, and later 8 wagons. In order to understand what is happening, a peak and a trough in the resonance diagram will be further elaborated. The results are compared to the prescription in the Eurocodes. All comparisons are made with the parameters determined in chapter 2 and 3. The moving oscillator is referred to as 1 DOF oscillator and the moving oscillator with rotational inertia is referred to as 2 DOF oscillator. Note that the deflections are amplified in the graphs for plotting reasons.

6.1 Importance of inertia

Determining the importance of inertia is the main research objective. Therefore, figure 6.1 compares the different vehicle models and shows the deflection of the middle of the bridges at two different velocities. Note that in some cases, the point load model, 1 DOF oscillator and 2 DOF oscillator show very similar results. This may lead to the three indistinguishable in the graphs.

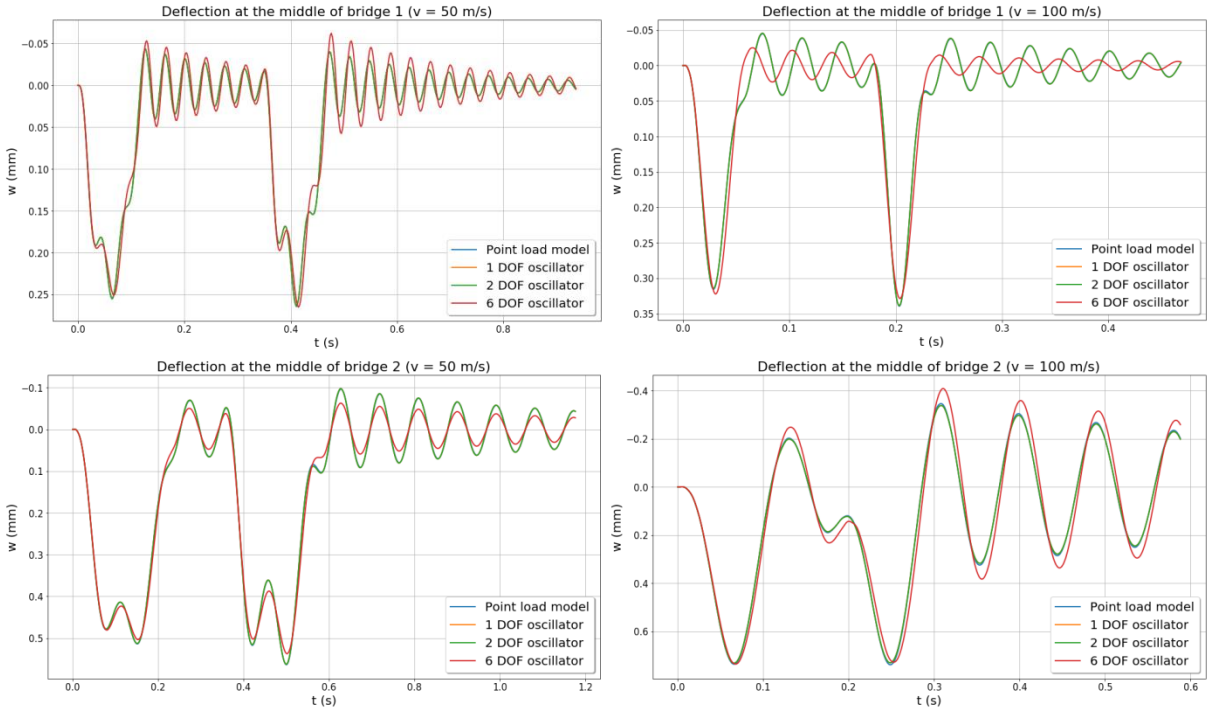

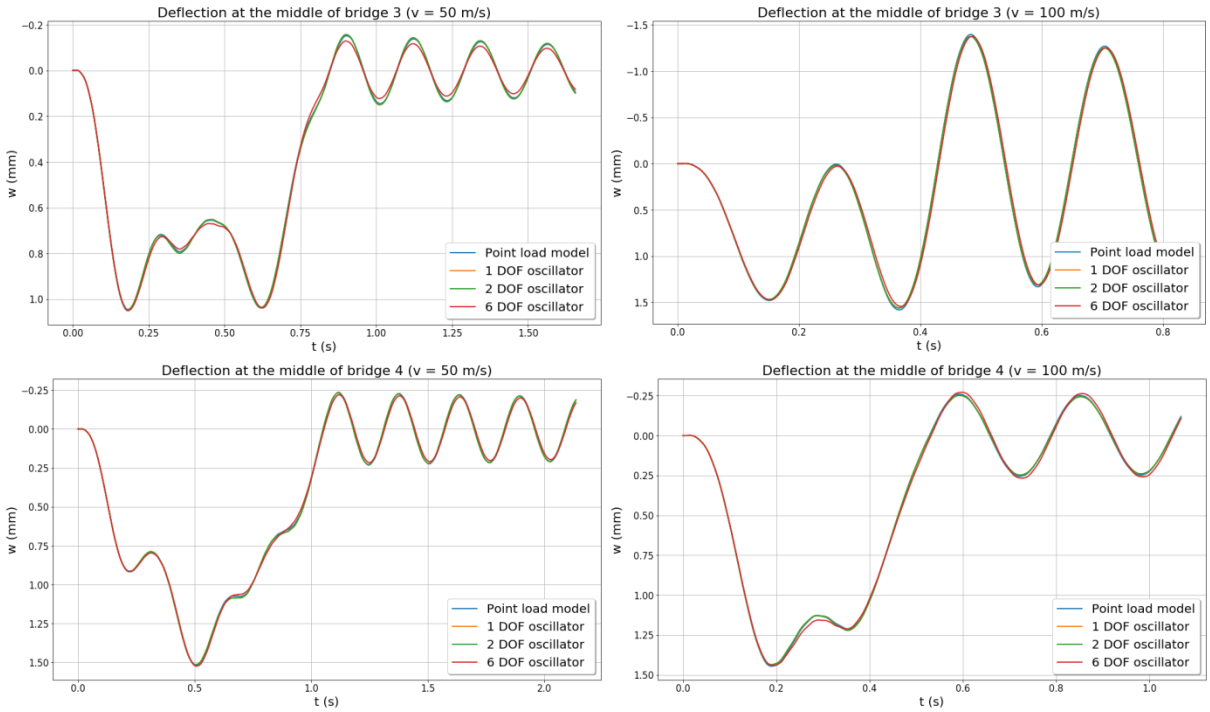

Figure 6.1: Bridge deflection with a single wagon

It becomes clear that the inertia and complexity of the vehicle model have a minimal impact on the magnitude of the deflections of the bridge. Only the most complex model shows a distinguishable difference. This can mainly be explained by the fact that that the bridge is stiff enough not to excite the inertia of the vehicle considerably. Incorporating the inertia into the model has small influence when compared to the model that accounts for a constant force due to gravity. Therefore, a change in the complexity of the vehicle has a minimal impact on the bridge.

To further investigate the importance of inertia, figure 6.2 makes a comparison of the deflections of the vehicle. To make the graphs clear, only the deflections of the front wheels are presented. The rear wheels show similar results.

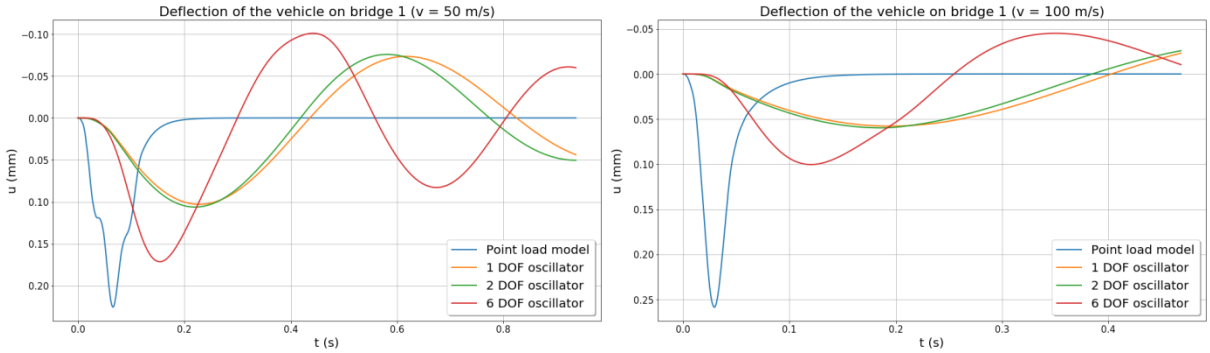

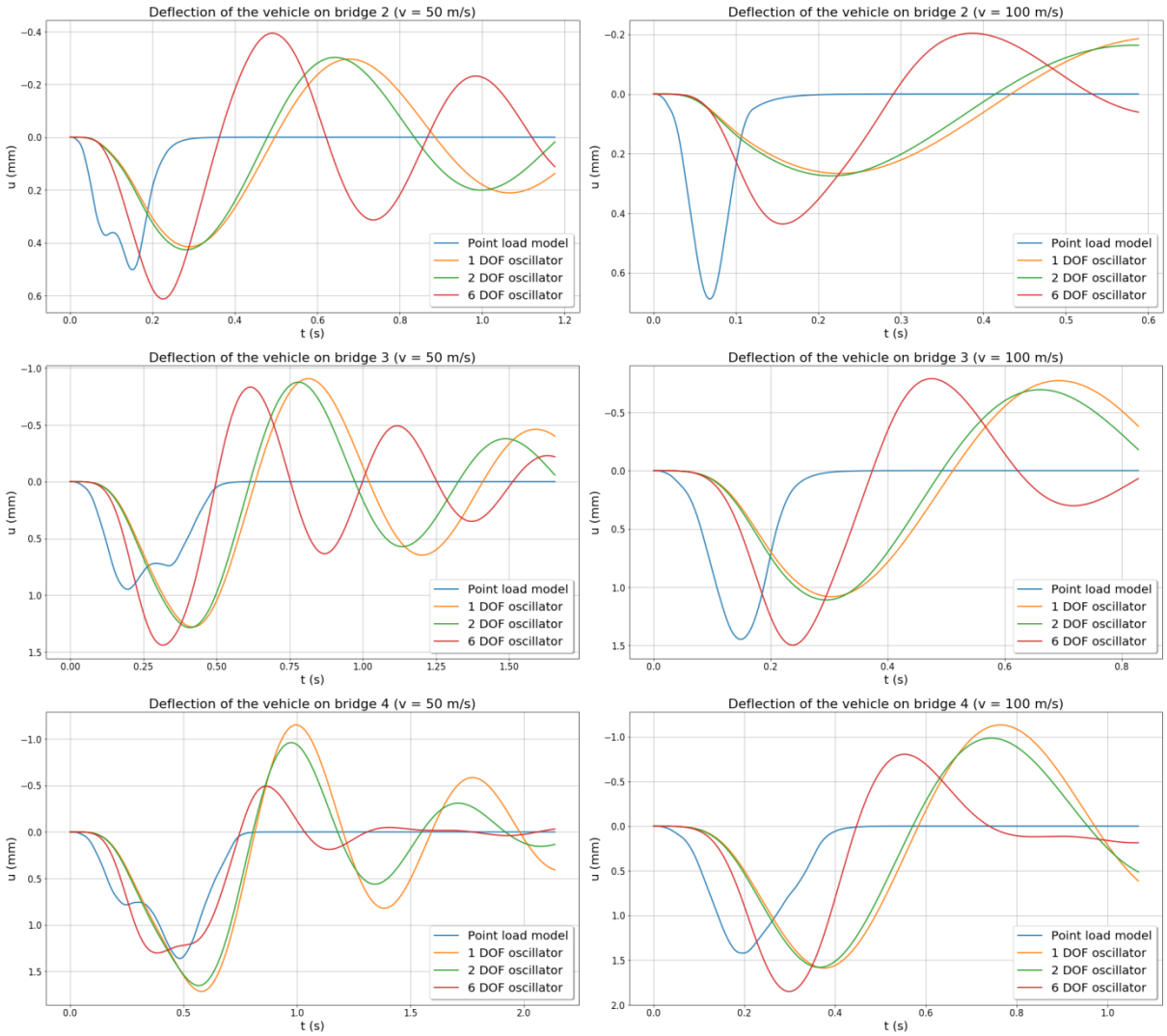

Figure 6.2: Vehicle deflection with a single wagon

The different vehicle models show interesting results. Where the moving point load follows the deflection of the beam, the more advanced models have a delayed response. The 1&2 DOF oscillators show similar results and are more delayed than the 6 DOF oscillator. Also the magnitude of the response differs: in most cases, the vehicle deflections of the 6 DOF oscillator are bigger, but this is not necessarily the case. Interestingly enough, the most complex 6 DOF model tends to be in between the moving point load and the 1&2 DOF oscillators. For both the delay and magnitude of the response, this can be explained: compared to the wagon itself, the wheels and bogies are fairly rigidly connected to the rails and bridge, which means that a part of the load behaves like a point load and another part behaves like an oscillator. Due to the relatively smaller oscillating mass, deflections tend to be bigger and responses are faster. However, the difference in magnitude of the vehicle response for each vehicle model differs for each bridge and velocity. This means that the influence of the complexity of the vehicle model strongly depends on the properties of the bridge and the velocity of the vehicle.

To further investigate the importance of inertia, tables 6.1 and 6.2 present the maximum values for the deflection and moments in the bridge, and deflections and vertical accelerations of the vehicle.

Table 6.1: Comparison of the models ($v = 50\ m/s$)

Model	Quantity	Bridge 1	Bridge 2	Bridge 3	Bridge 4	Unit
Point load model	w	0.26	0.57	1.05	1.52	mm
1 DOF oscillator	w	0.26	0.57	1.05	1.52	mm
2 DOF oscillator	w	0.26	0.57	1.05	1.51	mm
6 DOF oscillator	w	0.27	0.54	1.05	1.52	mm
Point load model	M	0.28	0.55	1.10	1.92	kNm
1 DOF oscillator	M	0.28	0.55	1.10	1.92	kNm
2 DOF oscillator	M	0.28	0.55	1.10	1.92	kNm
6 DOF oscillator	M	0.28	0.53	1.11	1.92	kNm
Point load model	u	0.23	0.55	1.04	1.36	mm
1 DOF oscillator	u	0.10	0.42	1.28	1.72	mm
2 DOF oscillator	u	0.11	0.45	1.34	1.80	mm
6 DOF oscillator	u	0.17	0.61	1.44	1.80	mm
Point load model	a	1.17	0.66	0.24	0.17	m/s^2
1 DOF oscillator	a	0.02	0.03	0.08	0.08	m/s^2
2 DOF oscillator	a	0.03	0.03	0.09	0.08	m/s^2
6 DOF oscillator	a	0.05	0.12	0.14	0.11	m/s^2

Table 6.2: Comparison of the models ($v = 100\ m/s$)

Model	Quantity	Bridge 1	Bridge 2	Bridge 3	Bridge 4	Unit
Point load model	w	0.34	0.74	1.58	1.45	mm
1 DOF oscillator	w	0.34	0.73	1.56	1.44	mm
2 DOF oscillator	w	0.34	0.73	1.56	1.44	mm
6 DOF oscillator	w	0.33	0.74	1.55	1.44	mm
Point load model	M	0.35	0.71	1.46	2.11	kNm
1 DOF oscillator	M	0.34	0.70	1.45	2.10	kNm
2 DOF oscillator	M	0.34	0.70	1.45	2.10	kNm
6 DOF oscillator	M	0.34	0.71	1.46	2.10	kNm
Point load model	u	0.29	0.71	1.45	1.42	mm
1 DOF oscillator	u	0.06	0.27	1.08	1.59	mm
2 DOF oscillator	u	0.07	0.30	1.11	1.58	mm
6 DOF oscillator	u	0.12	0.50	1.50	2.19	mm
Point load model	a	3.33	1.91	1.07	0.52	m/s^2
1 DOF oscillator	a	0.05	0.06	0.09	0.11	m/s^2
2 DOF oscillator	a	0.05	0.07	0.10	0.12	m/s^2
6 DOF oscillator	a	0.06	0.15	0.36	0.30	m/s^2

These tables show that for both the deflection and moments in the bridge, the complexity of the vehicle model does not have a significant impact. Again, this is due to the relatively stiff bridge. As opposed to the bridge, the vehicle itself shows large differences in deflections and vertical accelerations. The point load model follows the deflection of the bridge and shows unrealistically large values for the vertical accelerations of the vehicle. When a comparison is made between the moving oscillators, the 6 DOF model shows values up to three times larger for the vertical accelerations, compared to the 1&2 DOF oscillators. Thus, the 1&2 DOF oscillators strongly under evaluate the vertical accelerations of the vehicle.

6.2 Deflection of the wheels after passing the bridge

The model with six degrees of freedom has a bilinear spring implemented for the contact force between the wheels and the rails (equation 4.8). This means that a force is only applied in compression and the wheels can lose contact with the rails. These jumps only occur after the wheels have left the bridge. The largest magnitude is found for the front wheels, these are therefore presented in figure 6.3. Note that a negative value for u means that the wheel loses contact with the rails.

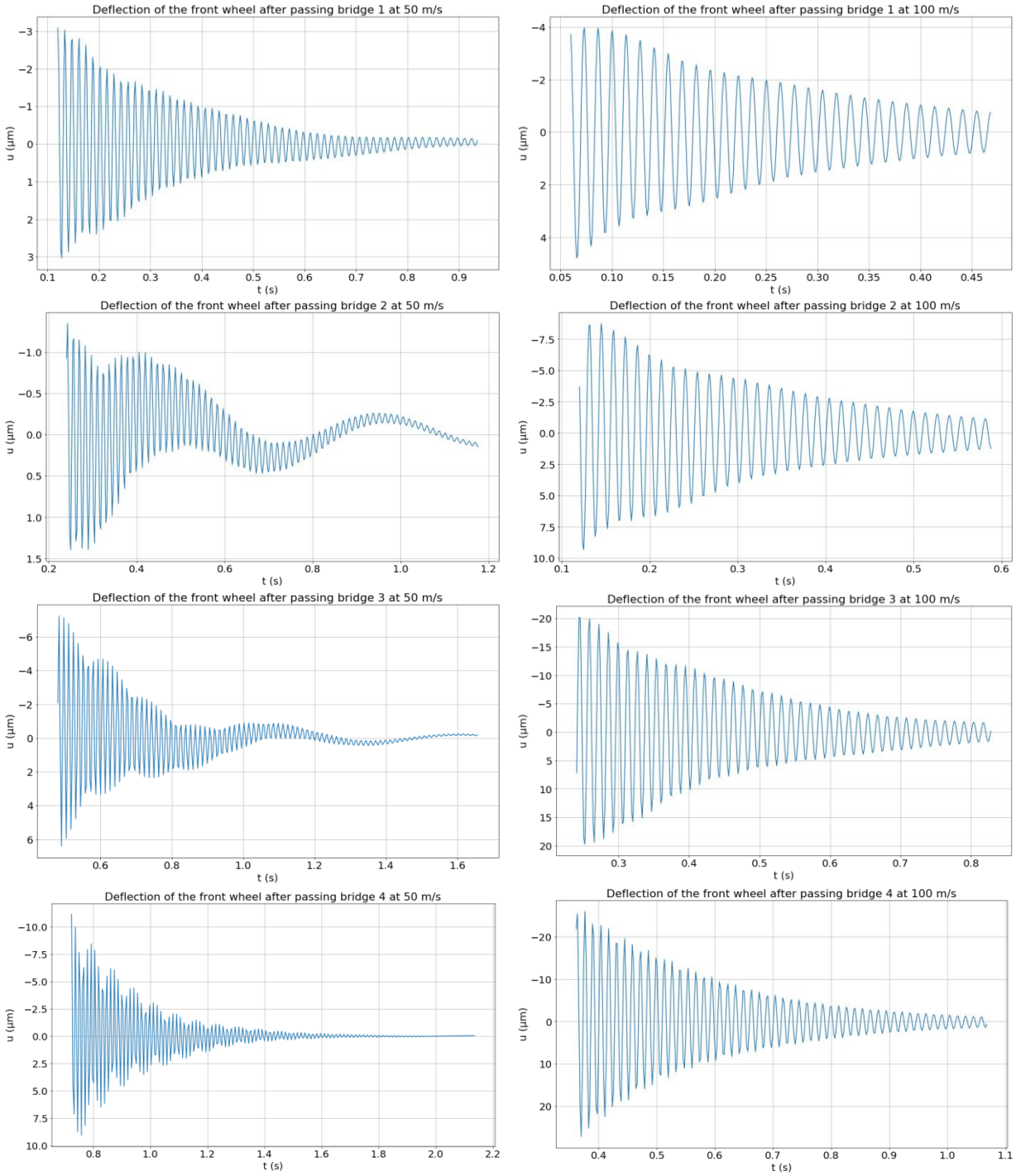

Figure 6.3: Deflection of the front wheels after passing the bridge

Figure 6.3 shows that the wheels do indeed lose contact with the rails. The magnitude of these jumps depends on the speed of the train and the bridge properties. The jumps are small: in the range from 1 to 25 μm, which would not be visible in reality. Also, the frequency of the contact loss is very high. This may lead to fatigue of the wheels and rails over time, but will not cause derailment.
It is striking that this only occurs after the wheels have left the bridge. Therefore, it is worth noting that the contact force between the wheels and rails is modelled as a bilinear spring, where the stiffness of both are taken into account. However, the foundation is assumed to be rigid, which means there is no dissipation of energy, and there is an unrealistically large track stiffness change experience by the moving vehicle when leaving the bridge. Also, the bridge is modelled as a simply supported beam, which is generally not the case for train bridges. Thus, in reality, the deflections over time may be different.

6.3 *Influence of the velocity*

The velocity of the vehicle is the easiest parameter to change, for example, in case of cracks in the bridge, or when deflections need diminishing. Therefore, the influence of the velocity on maximum deflections and moments in the bridge, and maximum vertical accelerations of the vehicle is assessed. To make a comparison, this is done for all models with a single wagon. The moments show very similar results to the deflection of the bridge. Therefore, only the deflections of the bridge over time are presented in the graphs on the left side. On the right side, vertical accelerations of the vehicle are presented.

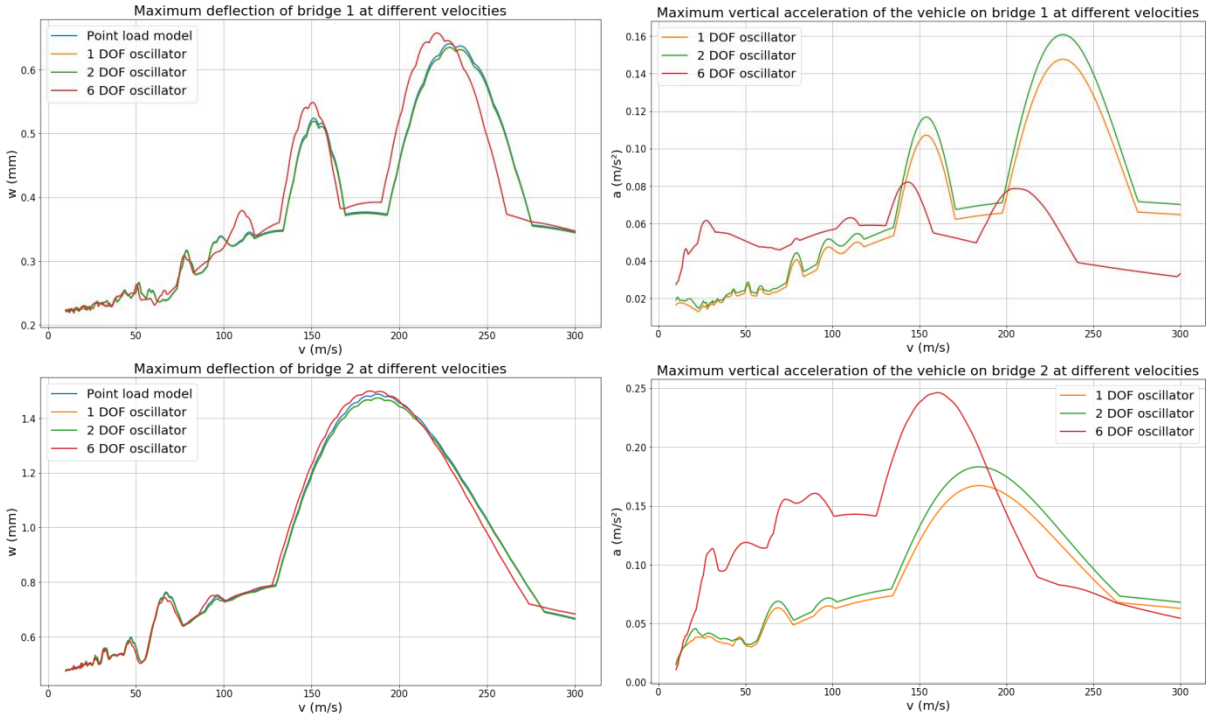

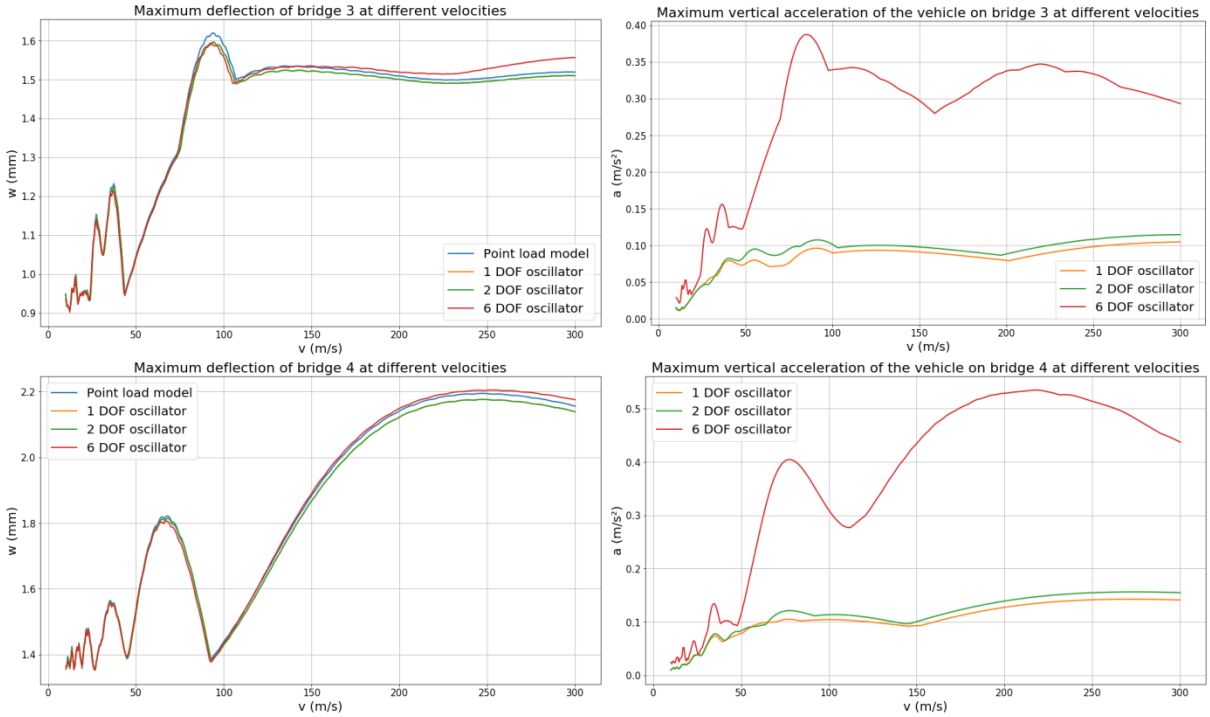

Figure 6.4: Influence of the velocity with a single wagon

Figure 6.4 shows that the influence of the velocity on the behaviour of the bridge and vehicle differs significantly for the parameters: resonance occurs at different velocities for every bridge. The influence of the different vehicle models on the bridge is minimal. However, it does have a considerable influence on the vertical accelerations of the vehicle itself. In most cases, the model with six degrees of freedom shows significantly higher vertical accelerations than the other two mass-spring systems. The simple point load model, which is not presented in the graphs, follows the deflection of the bridge and shows absurd vertical accelerations. This proofs the necessity of springs and dampers.

In reality, it is rarely the case that a single wagon crosses a bridge. Usually, a train consists of 8 wagons. Therefore, the behaviour of the bridge at different velocities is studied in this case as well. Since modelling multiple wagons leads to an increase in computation time and since the influence of the complexity of the model is negligible, only the bridge deflections in case of the moving point load model are computed. Figure 6.5 shows that for 8 wagons, peaks occur at different velocities, compared to a single wagon.

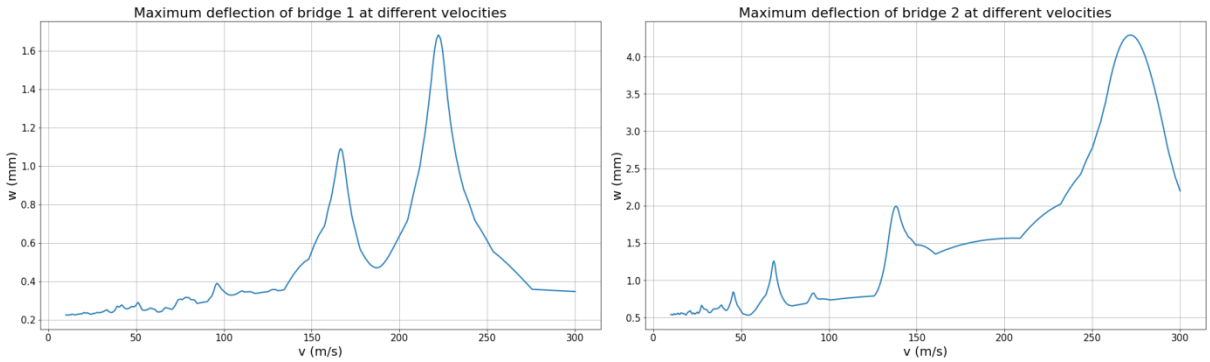

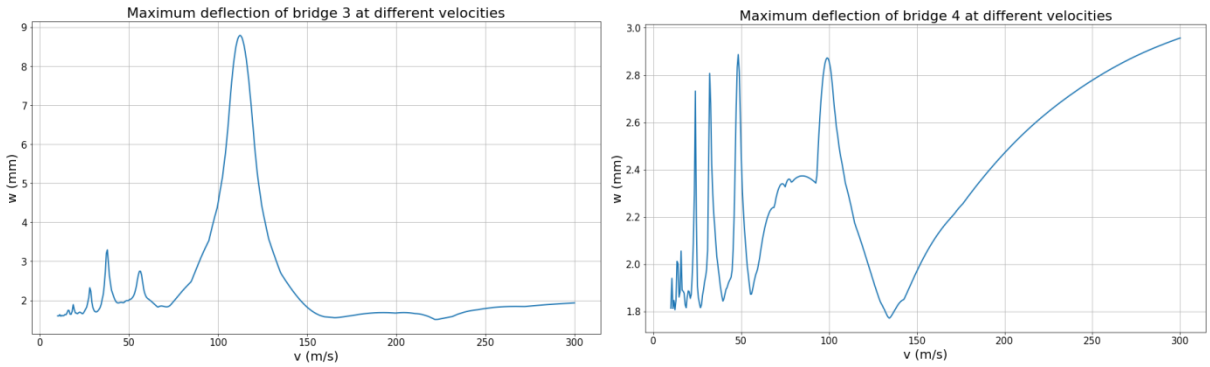

Figure 6.5: Influence of the velocity with 8 wagons (point load model only)

It strikes that bridge 3 shows a peak at 112.5 m/s. To understand what happens at this velocity, it is further examined and compared to a trough at 71.5 m/s. Therefore, figure 6.6 and table 6.3 show the difference of the bridge and vehicle deflection at these two velocities.

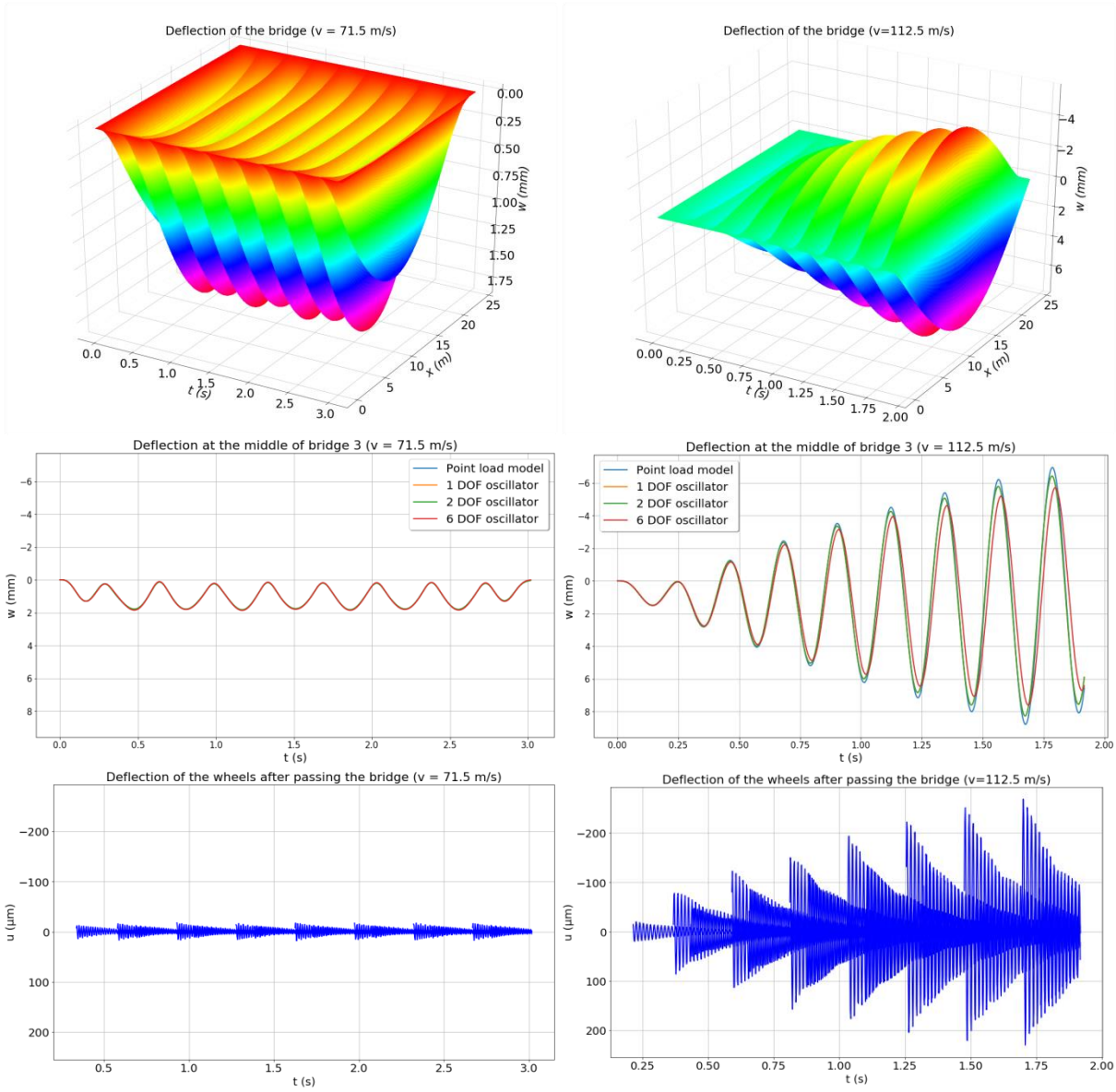

Figure 6.6: Comparison of bridge 3 with 8 wagons at different velocities.

Table 6.3: Comparison of bridge 3 at different velocities

Model	Quantity	$v = 71.5\ m/s$	$v = 112.5\ m/s$	Unit
Point load model	w	1.83	8.79	mm
1 DOF oscillator	w	1.83	8.28	mm
2 DOF oscillator	w	1.83	8.28	mm
6 DOF oscillator	w	1.86	7.61	mm
Point load model	M	1.66	8.12	kNm
1 DOF oscillator	M	1.66	7.64	kNm
2 DOF oscillator	M	1.66	7.64	kNm
6 DOF oscillator	M	1.69	7.03	kNm
Point load model	u	1.75	8.72	mm
1 DOF oscillator	u	1.86	4.15	mm
2 DOF oscillator	u	2.03	4.38	mm
6 DOF oscillator	u	2.38	5.01	mm
Point load model	a	0.47	7.30	m/s^2
1 DOF oscillator	a	0.13	0.61	m/s^2
2 DOF oscillator	a	0.15	0.66	m/s^2
6 DOF oscillator	a	0.37	1.81	m/s^2

It becomes clear that at 112.5 m/s resonance occurs and at 71.5 m/s some anti-resonance takes place. In case of resonance, the influence of the complexity of the vehicle on the bridge is marginal: the 6 DOF oscillator shows slightly smaller deflections. However, the influence of the complexity of the vehicle on the deflections and vertical accelerations of the vehicle itself are large. Vertical accelerations are three times higher in resonance for the most complex model, compared to the more simplistic models. The deflection of the wheels after passing the bridge in resonance increases for each wagon. This may lead to fatigue or derailment.

According to Graff, the first critical velocity at which resonance occurs should be $217.7\ m/s$ for moving point loads (Graff, 1975). This differs significantly from the results when 8 wagons are modelled. This is mainly due to the unequal distances between the wheels.

The Eurocodes prescribe, in case of train bridges, to perform the dynamic calculation with a static calculation and a dynamic loading factor for velocities below $200\ km/h$ (NEN, 2015). However, as shown in the graphs, resonance may occur at any velocity. This cannot be predicted with static calculations. When resonance occurs, the loading cannot be regarded as static. Therefore, the dynamic calculations are essential for understanding the behaviour of the bridge and the vehicle. Thus, it might be recommended to prescribe the dynamic calculations in the Eurocodes.

7 Conclusion and recommendations

The main goal of this thesis was to investigate and describe the interaction between a moving vehicle and a bridge. More specifically, the importance of the inertia of the vehicle for the serviceability limit state, and ultimate limit state was assessed. Therefore, a simply supported beam with different vehicle models was examined.

There can be concluded that inertia and the complexity of the vehicle model have a minimal influence on the deflections and moments in the bridge. This could be explained by the fact that that the bridge is stiff enough not to excite the inertia of the vehicle considerably. However, the complexity of the vehicle model has a significant impact on the displacements and vertical accelerations of the vehicle itself. The vehicle model with six degrees of freedom shows generally higher values for the deflections and vertical accelerations than the moving oscillator with one or two degrees of freedom. However, this is not always the case, because the influence of the complexity of the vehicle model strongly depends on the properties of the bridge and the velocity of the vehicle.
An advantage of the model with six degrees of freedom, is that the deflection of the wheels and wagons can be separately examined. This way, the deflections of the wheels show that, after the train leaves the bridge, the wheels make high frequency jumps on the rails of one hundredth of a millimetre. However, the bridge and track model lack in complexity. Therefore, more research needs to be performed to justify this finding.
Furthermore, the influence of the velocity on the displacements is large. This is mainly due to resonance of the bridge at critical velocities. At multiple velocities, the different vehicle models show similar results for the deflection of the bridge. The most complex model with six degrees of freedom shows again generally higher values for the vertical accelerations of the vehicle. When the length of the train is increased to multiple wagons, the results are different compared to a single wagon and resonance peaks can be found at different velocities. The Eurocodes prescribe a static calculation with a dynamic loading factor and disregards the resonance, which is an unsafe approach. According to the findings in this thesis, it might be recommended to prescribe the dynamic calculations in the Eurocodes.

In conclusion, neither inertia nor the complexity of the vehicle model have a significant impact on the ultimate limit state and serviceability limit state of the bridge. However, for the ultimate limit state and serviceability limit state of the vehicle the impact is large, and it could lead to the lack of comfort or derailment.

There are a few recommendations for further research. In this thesis, a single vehicle was modelled in one direction. The interaction of multiple vehicles driving in two directions leads to torsion and may affect the vertical accelerations and stresses. For torsion to be possible, a torsional degree of freedom should be added or a plate should be considered. In that case, an Euler-Bernoulli beam is not sufficient. In the bridge model, a simply supported beam was chosen. For further research, it is advisable to investigate more advance bridge models, for example, a continuously supported beam. The scope of this thesis is limited to vehicle induced vibrations on a bridge, while often, subsidence of the substrate occurs close to bridges. This would lead to a non-zero initial stress state and non-zero initial conditions. Further research in this direction may lead to interesting results.

8 References

Arvidsson T., Karoumi R. and Pacoste C. Statistical screening of modelling alternatives in train-bridge interaction systems. Engineering Structures, vol.59, 2014, pages 693-701.

Canetta D. Le Prospettive della Trazione Ferroviaria per gli Anni 2020-2030. Bombardier, The evolution of mobility, 2017.

EN 1990:2002/A1:2005, Eurocode-Basis of structural design, Final Draft, European Committee for standardization, CEN, 2006.

Graaf, de, A. Theoretical model and application of a damped two degree of freedom spring-mass system, moving across a simply supported beam, 2018. Retrieved from https://repository.tudelft.nl/

Graff, K.F., Wave Motion in Elastic Solids. Dover publications, New York. Page 744.

J. R. Ravetz, The Rational Mechanics of Flexible or Elastic Bodies. C. Truesdell, Isis 53, no. 2, 1962, pages 263-266.

Martínez-Castro, A.E., García-Macías, E., Train-speed sensitivity approach for maximum response envelopes in dynamics of railway bridges, Journal of Sound and Vibration, Volume 452, 2019, pages 13-33.

Ouchene, B. Dynamische interactie tussen een bewegende massa-veer systeem en een buigligger, 2017. Retrieved from https://repository.tudelft.nl/

Tee USA, News and New Arrivals, 2007. Retrieved from https://www.tee-usa.com/

Timoshenko, Stephen, Young. Vibration Problems in Engineering, by S. Timoshenko. Princeton, N.J.: Van Nostrand, 1961.

Wikipedia, Bogie, 2018. Retrieved from https://en.wikipedia.org/wiki/Bogie

Yang, Y.B., Yau, J.D., Wu, Y.S., Vehicle-Bridge Interaction Dynamics. Journal of Sound and Vibration, Volume 278, Issues 4–5, 2004, pages 20-26

Appendix A: Analytical solution

In this appendix, the Euler-Bernoulli beam equation is used to determine the behaviour of the bridge. First, we will solve the homogeneous equation to determine the behaviour of the bridge when there are no forces applied. Then we will solve the particular equation, to determine the behaviour when external forces are applied.

The Euler-Bernoulli beam equation is shown in formula A.1, also the external loading is specified. First, we will solve the homogeneous equation, which is presented in equation A.2.

$$\begin{aligned} EI\frac{\partial^4 w}{\partial x^4}(x,t) + c_d I\frac{\partial^5 w}{\partial x^4 \partial t}(x,t) + \rho A\frac{\partial^2 w}{\partial t^2}(x,t) &= q(x,t) \\ q(x,t) = \sum_i Q_i(t)\cdot\delta\big(x-(vt_i)\big)\cdot H(vt-s_i)\cdot H\big(l-(vt_i)\big) & \end{aligned} \tag{A.1}$$

$$EI\frac{\partial^4 w}{\partial x^4}(x,t) + c_d I\frac{\partial^5 w}{\partial x^4 \partial t}(x,t) + \rho A\frac{\partial^2 w}{\partial t^2}(x,t) = 0 \tag{A.2}$$

To solve for the homogeneous solution, the separation of variables will be applied, as shown in equations A.3 and A.4. Note that in equation A.4 the left hand side is only dependent of x and the right hand side is only dependent of time. Hence, both sides of the equation are constant. Also, in equation A.5 the boundary conditions can only be applied on $w_x(x)$, since applying them on w_t(t) will lead to the trivial solution.

$$w(x,t) = w_x(x)\cdot w_t(t) \tag{A.3}$$

$$\frac{\frac{\partial^4 w_x}{\partial x^4}(x)}{w_x(x)} = -\frac{\rho A}{E}\cdot\frac{\frac{\partial^2 w_t}{\partial t^2}(t)}{w_t(t)+\frac{c_d}{E}\frac{\partial w}{\partial t}(t)} = \eta \tag{A.4}$$

$$\begin{aligned} w_x(0) &= 0 & \frac{\partial^2 w_x}{\partial x^2}(0) &= 0 \\ w_x(l) &= 0 & \frac{\partial^2 w_x}{\partial x^2}(l) &= 0 \end{aligned} \tag{A.5}$$

From equation A.4, two differential equations are derived, the first one is stated in equation A.6. For η it is possible to substitute $\eta = -{\beta_n}^4 < 0$, $\eta = 0$ or $\eta = {\beta_n}^4 > 0$. Only the last one will lead to a non-trivial solution. The solution to equation A.6, taking into account boundary conditions, is shown in equation A.7.

$$\begin{aligned} \frac{\partial^4 w_x}{\partial x^4}(x) - \eta\cdot w_x(x) &= 0 \\ \frac{\partial^2 w_t}{\partial t^2}(t) + \frac{EI}{\rho A}\eta\cdot\left(w_t(t)-\frac{c_d}{E}\frac{\partial w}{\partial t}(t)\right) &= 0 \end{aligned} \tag{A.6}$$

$$
\begin{aligned}
w_{xn}(x) &= C_n \cdot \sin(\beta_n x) \\
w_x(x) &= \sum_{n=1}^{\infty} C_n \cdot \sin(\beta_n x) \\
\beta_n &= \frac{n\pi}{l} \text{ (with } n = 1, 2, 3, \dots)
\end{aligned}
\tag{A.7}
$$

When applying the same value for η, we can solve for the differential equation of w_{tn}, as shown in equation A.8. Note that the eigen frequency ω_n, follows naturally from the equation. The solution is show in equation A.9.

$$
\begin{aligned}
\frac{\partial^2 w_{tn}}{\partial t^2}(t) + 2\zeta\omega_n \frac{\partial w_{tn}}{\partial t}(t) + {\omega_n}^2 w_{tn}(t) &= 0 \\
\omega_n &= \sqrt{\frac{EI}{\rho A}}\left(\frac{n\pi}{l}\right)^2 \\
\zeta &= \frac{c_d I}{2\sqrt{EI\ \rho A}}\left(\frac{n\pi}{l}\right)^2
\end{aligned}
\tag{A.8}
$$

$$
\begin{aligned}
w_{tn}(t) &= (C_n\ \sin(\omega_n t) + D_n\ \cos(\omega_n t))e^{-\zeta\omega_n t} \\
w_t(t) &= \sum_{n=1}^{\infty} (C_n\ \sin(\omega_n t) + D_n\ \cos(\omega_n t))\, e^{-\zeta\omega_n t}
\end{aligned}
\tag{A.9}
$$

Now that both the x and time dependent part are know, we can combine both in the homogeneous solution, as is shown in equation A.10.

$$
\begin{aligned}
w_n(x,t) &= \sin(\beta x) \cdot (C_n \cdot \sin(\omega_n t) + D_n \cdot \cos(\omega_n t))e^{-\zeta\omega_n t} \\
w(x,t) &= \sum_{n=1}^{\infty} \sin(\beta x) \cdot (C_n \cdot \sin(\omega_n t) + D_n \cdot \cos(\omega_n t))\, e^{-\zeta\omega_n t}
\end{aligned}
\tag{A.10}
$$

Now, we will solve for the particular solution. It is assumed that the x-dependant part of the bending in the particular solution is the same as in the homogeneous solution. This is reasonable since it meets the homogeneous boundary conditions. The time-dependent part is still unknown. The particular equation is shown in equation A.11, also the external loading is specified.

$$
\begin{aligned}
EI\frac{\partial^4 w}{\partial x^4}(x,t) + c_d I\frac{\partial^5 w}{\partial x^4 \partial t}(x,t) + \rho A\frac{\partial^2 w}{\partial t^2}(x,t) &= q(x,t) \\
q(x,t) &= \sum_i Q_i(t) \cdot \delta(x - vt_i) \cdot H(vt_i) \cdot H(l - vt_i)
\end{aligned}
\tag{A.11}
$$

After applying again the separation of variables, as show in equation A.3, the equation can be written as follows.

$$
EI\frac{\partial^4 w_x}{\partial x^4}(x) \cdot w_t(t) + c_d I\frac{\partial^4 w_x}{\partial x^4}(x) \cdot \frac{\partial w_t}{\partial t}(t) + \rho A\, w_x(x) \cdot \frac{\partial^2 w_t}{\partial t^2}(t) = q(x,t) \tag{A.12}
$$

After substituting equation A.13 in A.12, equation A.14 is found.

$$\begin{gathered} w_{xn}(x) = \sin(\beta_n x) \\ \frac{\partial^4 w_{xn}}{\partial x^4}(x) = {\beta_n}^4 \sin(\beta_n x) \\ \frac{\partial^4 w_{xn}}{\partial x^4}(x) = {\beta_n}^4 w_{xn}(x) \end{gathered} \tag{A.13}$$

$$\left(\rho A \frac{\partial^2 w_t}{\partial t^2}(t) + EI\ {\beta_n}^4 \cdot \left(w_t(t) - \frac{c_d}{E}\frac{\partial w}{\partial t}(t)\right)\right) \cdot \sin(\beta_n x) = q(x,t) \tag{A.14}$$

Due to orthogonality, the second order differential equation can be found (equation A.15-A.17).

$$\left(\frac{\partial^2 w_t}{\partial t^2}(t) + 2\zeta\omega_n \frac{\partial w_{tn}}{\partial t}(t) + {\omega_n}^2\, w_t(t)\right) \cdot \sin^2(\beta_n x) = \frac{q(x,t)}{\rho A} \cdot \sin(\beta_n x) \tag{A.15}$$

$$\left(\frac{\partial^2 w_t}{\partial t^2}(t) + 2\zeta\omega_n \frac{\partial w_{tn}}{\partial t}(t) + {\omega_n}^2\, w_t(t)\right) \cdot \int_0^l \sin^2(\beta_n x)\ dx = \int_0^l \frac{q(x,t)}{\rho A} \cdot \sin(\beta_n x)\ dx \tag{A.16}$$

$$\frac{\partial^2 w_t}{\partial t^2}(t) + 2\zeta\omega_n \frac{\partial w_{tn}}{\partial t}(t) + {\omega_n}^2\, w_t(t) = \frac{2}{\rho A l} \cdot \int_0^l \sin(\beta_n x) \cdot q(x,t)\ dx \tag{A.17}$$

After integrating the right hand side, the following differential equation A.18 is derived. This differential equation is solved numerically for complex loads, which is specified in Appendix B. The general total solution is presented in equation A.19.

$$\begin{gathered} \frac{\partial^2 w_{tn}}{\partial t^2}(t) + 2\zeta\omega_n \frac{\partial w_{tn}}{\partial t}(t) + {\omega_n}^2\, w_{tn}(t) = \sum_i f_n(vt_i) \cdot Q_i(t) \\ f_n(vt) = \frac{2\ \sin(\beta_n\, vt)}{\rho A l} \cdot H(vt) \cdot H(l - vt) \end{gathered} \tag{A.18}$$

$$w(x,t) = \sum_{n=1}^{\infty} w_{xn}(x) \cdot w_{tn}(t) \tag{A.19}$$

For a simple point load without damping, this equation can be solve analytically. This is done by Graff, as shown in equation A.20 (Graff, 1975).

$$w(x,t) = \frac{2Q}{\rho A l} \sum_{n=1}^{\infty} \frac{\sin(\beta_n x)}{\omega_n\left({\beta_n}^2 v^2 - {\omega_n}^2\right)} \left(\beta_n v \sin(\omega_n\, t) - \omega_n \sin(\beta_n\, vt)\right) \tag{A.20}$$

Appendix B: Numerical models in state-space representation

Introduction

This appendix covers the translation of the numerical models to differential equations in state-space representation, which can be solved with for example Python. The input of all models consists of the initial conditions in vector y_0, and the output is the derivative of the time dependant deflections, vector $\dot{y}$. Note that all the models only consist of the time-dependant part of the deflection. The solution still has to be multiplied by the x-dependant part, as specified in chapter 3. A side note should be added that for the relative vertical velocity of the vehicle and the bridge, there is not accounted for the influence of the horizontal velocity of the vehicle (equations B.3, B.6, B.B.13, B.14, B.27, B.28).

Moving point load model

The first model is not covered in the main report. It consists of moving point loads on the bridge, which are independent of de deflection. The time-dependant part of the deflection is stored in a vector y with length $2N$, as shown in equation B.1. The time derivative of y can then be computed, this is done in equations B.2 and B.3. To complete the model, initial conditions are shown in equation B.4.

$$\begin{aligned}
w_{t1}(t) &= y_1 \\
\dot{w}_{t1}(t) &= y_2 \\
\ddot{w}_{t1}(t) &= \dot{y}_2 \\
&\vdots \\
w_{tn}(t) &= y_{2n-1} \\
\dot{w}_{tn}(t) &= y_{2n} \\
\ddot{w}_{tn}(t) &= \dot{y}_{2n} \\
&\vdots \\
w_{tN}(t) &= y_{2N-1} \\
\dot{w}_{tN}(t) &= y_{2N} \\
\ddot{w}_{tN}(t) &= \dot{y}_{2N}
\end{aligned} \tag{B.1}$$

$$\begin{aligned}
\dot{y}_{2n-1} &= \dot{w}_{tn}(t) \\
\dot{y}_{2n-1} &= y_{2n}
\end{aligned} \tag{B.2}$$

$$\begin{aligned}
\ddot{w}_{tn}(t) + {\omega_n}^2\, w_{tn}(t) &= \sum_i f_n(vt_i) \cdot Q_i \\
\dot{y}_{2n} &= \sum_i f_n(vt_i) \cdot Q_i - {\omega_n}^2\, y_{2n-1}
\end{aligned} \tag{B.3}$$

$$\begin{aligned}
w_{tn}(0) &= 0 & \qquad y_{2n-1,0} &= 0 \\
\dot{w}_{tn}(0) &= 0 & \qquad y_{2n,0} &= 0
\end{aligned} \tag{B.4}$$

Moving oscillator

The previous model can be expanded with more degrees of freedom. The next model consists of moving oscillators on the beam, which are dependent of de deflection of the beam and vehicle itself. Equations B.5 shows the definition of the vector y, which is expanded with the deflection of the vehicle(s). Equation B.6 specifies the value of the force between the bridge and vehicle. Note that a force in compression is positive. Equations B.7-B.10 specify every value for the time derivative of y, and B.11 show the initial conditions.

$$\begin{aligned} w_{t1}(t) &= y_1 & u_1(t) &= y_{2N+1} \\ \dot{w}_{t1}(t) &= y_2 & \dot{u}_1(t) &= y_{2N+2} \\ \ddot{w}_{t1}(t) &= \dot{y}_2 & \ddot{u}_1(t) &= \dot{y}_{2N+2} \\ &\vdots & &\vdots \\ w_{tn}(t) &= y_{2n-1} & u_i(t) &= y_{2N+2i-1} \\ \dot{w}_{tn}(t) &= y_{2n} & \dot{u}_i(t) &= y_{2N+2i} \\ \ddot{w}_{tn}(t) &= \dot{y}_{2n} & \ddot{u}_i(t) &= \dot{y}_{2N+2i} \\ &\vdots & &\vdots \\ w_{tN}(t) &= y_{2N-1} & u_I(t) &= y_{2N+2I-1} \\ \dot{w}_{tN}(t) &= y_{2N} & \dot{u}_I(t) &= y_{2N+2I} \\ \ddot{w}_{tN}(t) &= \dot{y}_{2N} & \ddot{u}_I(t) &= \dot{y}_{2N+2I} \end{aligned} \tag{B.5}$$

$$\begin{aligned} Q_i(t) &= k\left(u_i(t) - \sum_{n=1}^{N} w_{tn}(t)\, w_{xn}(vt)\right) + c\left(\dot{u}_i(t) - \sum_{n=1}^{N} \dot{w}_{tn}(t)\, w_{xn}(vt)\right) \\ Q_i(t) &= k\left(y_{2N+2i-1} - \sum_{n=1}^{N} y_{2n-1}\, \sin(\beta_n\, vt)\right) + c\left(y_{2N+2i} - \sum_{n=1}^{N} y_{2n}\, \sin(\beta_n\, vt)\right) \end{aligned} \tag{B.6}$$

$$\begin{aligned} \dot{y}_{2n-1} &= \dot{w}_{tn}(t) \\ \dot{y}_{2n-1} &= y_{2n} \end{aligned} \tag{B.7}$$

$$\begin{aligned} \ddot{w}_{tn}(t) + {\omega_n}^2\, w_{tn}(t) &= \sum_i f_n(vt_i) \cdot Q_i\,(t) \\ \dot{y}_{2n} &= \sum_i f_n(vt_i) \cdot Q_i\,(t) - {\omega_n}^2\, y_{2n-1} \end{aligned} \tag{B.8}$$

$$\begin{aligned} \dot{y}_{2N+2i-1} &= \dot{u}_i(t) \\ \dot{y}_{2N+2i-1} &= y_{2N+2i} \end{aligned} \tag{B.9}$$

$$\begin{aligned} m\ddot{u}(t) &= mg - Q(t) \\ \dot{y}_{2N+2i} &= -\frac{1}{m}\sum_i Q_i(t) + g \end{aligned} \tag{B.10}$$

$$\begin{aligned} w_{tn}(0) &= 0 & y_{2n-1,0} &= 0 \\ \dot{w}_{tn}(0) &= 0 & y_{2n,0} &= 0 \\ u(0) &= \frac{mg}{2k} & y_{2N+4i-3,0} &= \frac{mg}{2k} \\ \dot{u}(0) &= 0 & y_{2N+4i-2,0} &= 0 \end{aligned} \tag{B.11}$$

Moving oscillator with rotational inertia

Also this model can be expanded with more degrees of freedom. The next model consists of moving oscillators with rotational inertia. Equations B.12 shows the definition of the vector y, which is expanded with the rotation of the vehicle(s). Equations B.13 and B.14 specify the value for the forces between the bridge and vehicle. Equations B.15-B.20 specify every value for the time derivative of y, and B.21 shows the initial conditions.

$$\begin{array}{lll}
w_{t1}(t) = y_1 & u_1(t) = y_{2N+1} & \theta_1(t) = y_{2N+3} \\
\dot{w}_{t1}(t) = y_2 & \dot{u}_1(t) = y_{2N+2} & \dot{\theta}_1(t) = y_{2N+4} \\
\ddot{w}_{t1}(t) = \dot{y}_2 & \ddot{u}_1(t) = \dot{y}_{2N+2} & \ddot{\theta}_1(t) = \dot{y}_{2N+4} \\
\vdots & \vdots & \vdots \\
w_{tn}(t) = y_{2n-1} & u_i(t) = y_{2N+4i-3} & \theta_i(t) = y_{2N+4i-1} \\
\dot{w}_{tn}(t) = y_{2n} & \dot{u}_i(t) = y_{2N+4i-2} & \dot{\theta}_i(t) = y_{2N+4i} \\
\ddot{w}_{tn}(t) = \dot{y}_{2n} & \ddot{u}_i(t) = \dot{y}_{2N+4i-2} & \ddot{\theta}_i(t) = \dot{y}_{2N+4i} \\
\vdots & \vdots & \vdots \\
w_{tN}(t) = y_{2N-1} & u_I(t) = y_{2N+4I-3} & \theta_I(t) = y_{2N+4I-1} \\
\dot{w}_{tN}(t) = y_{2N} & \dot{u}_I(t) = y_{2N+4I-2} & \dot{\theta}_I(t) = y_{2N+4I} \\
\ddot{w}_{tN}(t) = \dot{y}_{2N} & \ddot{u}_I(t) = \dot{y}_{2N+4I-2} & \ddot{\theta}_I(t) = \dot{y}_{2N+4I}
\end{array} \tag{B.12}$$

$$\begin{aligned}
Q_{iL}(t) = k\left(u_i(t) + \frac{1}{2}b\,\theta_i(t) - \sum_{n=1}^{N} w_{tn}(t)\,w_{xn}(vt_i - b)\right) \\
+ c\left(\dot{u}_i(t) + \frac{1}{2}b\,\dot{\theta}_i(t) - \sum_{n=1}^{N} \dot{w}_{tn}(t)\,w_{xn}(vt_i - b)\right) \\
Q_{iL}(t) = k\left(y_{2N+4i-3}(t) + \frac{1}{2}b\,y_{2N+4i-1}(t) - \sum_{n=1}^{N} w_{tn}(t)\,w_{xn}(vt_i - b)\right) \\
+ c\left(y_{2N+4i-2} + \frac{1}{2}b\,y_{2N+4i} - \sum_{n=1}^{N} \dot{w}_{tn}(t)\,w_{xn}(vt_i - b)\right)
\end{aligned} \tag{B.13}$$

$$\begin{aligned}
Q_{iR}(t) = k\left(u_i(t) - \frac{1}{2}b\,\theta_i(t) - \sum_{n=1}^{N} w_{tn}(t)\,w_{xn}(vt_i)\right) \\
+ c\left(\dot{u}_i(t) - \frac{1}{2}b\,\dot{\theta}_i(t) - \sum_{n=1}^{N} \dot{w}_{tn}(t)\,w_{xn}(vt_i)\right) \\
Q_{iR}(t) = k\left(y_{2N+4i-3}(t) - \frac{1}{2}b\,y_{2N+4i-1}(t) - \sum_{n=1}^{N} w_{tn}(t)\,w_{xn}(vt_i)\right) \\
+ c\left(y_{2N+4i-2} - \frac{1}{2}b\,y_{2N+4i} - \sum_{n=1}^{N} \dot{w}_{tn}(t)\,w_{xn}(vt_i)\right)
\end{aligned} \tag{B.14}$$

$$\begin{aligned}
\dot{y}_{2n-1} = \dot{w}_{tn}(t) \\
\dot{y}_{2n-1} = y_{2n}
\end{aligned} \tag{B.15}$$

$$\ddot{w}_{tn}(t) + {\omega_n}^2\, w_{tn}(t) = \sum_i \big(f_n(vt - s_i - b)\cdot Q_{iL}(t) + f_n(vt_i)\cdot Q_{iR}(t)\big)$$
$$\dot{y}_{2n} = \sum_i \big(f_n(vt_i - b)\cdot Q_{iL}(t) + f_n(vt_i)\cdot Q_{iR}(t)\big) - {\omega_n}^2\, y_{2n-1} \tag{B.16}$$

$$\dot{y}_{2N+4i-3} = \dot{u}_i(t)$$
$$\dot{y}_{2N+4i-3} = y_{2N+4i} \tag{B.17}$$

$$m\ddot{u}(t) = mg - Q_L(t) - Q_R(t)$$
$$\dot{y}_{2N+2i} = -\frac{1}{m}\sum_i \big(Q_{iL}(t) + Q_{iR}(t)\big) + g \tag{B.18}$$

$$\dot{y}_{2N+4i-1} = \dot{\theta}(t)$$
$$\dot{y}_{2N+4i-1} = y_{2N+4i} \tag{B.19}$$

$$J\ddot{\theta}(t) = \frac{b}{2}\big(-Q_{iL}(t) + Q_{iR}(t)\big)$$
$$\dot{y}_{2N+4i} = \frac{b}{2J}\big(-Q_{iL}(t) + Q_{iR}(t)\big) \tag{B.20}$$

$$\begin{aligned} w_{tn}(0) &= 0 & y_{2n-1,0} &= 0 \\ \dot{w}_{tn}(0) &= 0 & y_{2n,0} &= 0 \\ u(0) &= \frac{mg}{2k} & y_{2N+4i-3,0} &= \frac{mg}{2k} \\ \dot{u}(0) &= 0 & y_{2N+4i-2,0} &= 0 \\ \theta(0) &= 0 & y_{2N+4i-1,0} &= 0 \\ \dot{\theta}(0) &= 0 & y_{2N+4i,0} &= 0 \end{aligned} \tag{B.21}$$

Moving oscillator with six degrees of freedom

The final and most complex model consists of moving oscillators on the bridge, with six degrees of freedom and a bilinear spring stiffness between the wheels and the bridge. This way, a force can only be applied in compression and the wheel can come loose from the beam. Equations B.22 shows the definition of the vector y, which is expanded with the deflection of all parts of the vehicle. Equations B.23-B.28 specify the value for the forces between the beam and vehicle and the forces within the vehicle itself. Equations B.29-B.42 specify every value for the time derivative of y, and B.43 show the initial conditions.

$$
\begin{array}{lll}
w_{t1}(t) = y_1 & u_{1,1}(t) = y_{2N+1} & \theta_1(t) = y_{2N+3} \\
\dot{w}_{t1}(t) = y_2 & \dot{u}_{1,1}(t) = y_{2N+2} & \dot{\theta}_1(t) = y_{2N+4} \\
\vdots & \vdots & \vdots \\
w_{tn}(t) = y_{2n-1} & u_{i,1}(t) = y_{2N+12i-11} & \theta_i(t) = y_{2N+12i-9} \\
\dot{w}_{tn}(t) = y_{2n} & \dot{u}_{i,1}(t) = y_{2N+12i-10} & \dot{\theta}_i(t) = y_{2N+12i-8} \\
\vdots & \vdots & \vdots \\
w_{tN}(t) = y_{2N-1} & u_{I,1}(t) = y_{2N+12I-11} & \theta_I(t) = y_{2N+12I-9} \\
\dot{w}_{tN}(t) = y_{2N} & \dot{u}_{I,1}(t) = y_{2N+12I-10} & \dot{\theta}_I(t) = y_{2N+12I-8}
\end{array}
$$

$$
\begin{array}{ll}
u_{1,2L}(t) = y_{2N+5} & u_{1,2R}(t) = y_{2N+7} \\
\dot{u}_{1,2L}(t) = y_{2N+6} & \dot{u}_{1,2R}(t) = y_{2N+8} \\
\vdots & \vdots \\
u_{i,2L}(t) = y_{2N+12i-7} & u_{i,2R}(t) = y_{2N+12i-5} \\
\dot{u}_{i,2L}(t) = y_{2N+12i-6} & \dot{u}_{i,2R}(t) = y_{2N+12i-4} \\
\vdots & \vdots \\
u_{I,2L}(t) = y_{2N+12I-7} & u_{I,2R}(t) = y_{2N+12I-5} \\
\dot{u}_{I,2L}(t) = y_{2N+12I-6} & \dot{u}_{I,2R}(t) = y_{2N+12I-4}
\end{array}
$$

$$
\begin{array}{ll}
u_{1,3L}(t) = y_{2N+9} & u_{1,3R}(t) = y_{2N+11} \\
\dot{u}_{1,3L}(t) = y_{2N+10} & \dot{u}_{1,3R}(t) = y_{2N+12} \\
\vdots & \vdots \\
u_{i,3L}(t) = y_{2N+12i-3} & u_{i,3R}(t) = y_{2N+12i-1} \\
\dot{u}_{i,3L}(t) = y_{2N+12i-2} & \dot{u}_{i,3R}(t) = y_{2N+12i} \\
\vdots & \vdots \\
u_{I,3L}(t) = y_{2N+12I-3} & u_{I,3R}(t) = y_{2N+12I-1} \\
\dot{u}_{I,3L}(t) = y_{2N+12I-2} & \dot{u}_{I,3R}(t) = y_{2N+12I}
\end{array}
\qquad \text{(B.22)}
$$

$$Q_{i,1L}(t) = k_1\left(u_{i,1}(t) + \frac{1}{2}b\,\theta_i(t) - u_{i,2L}\right) + c_1\left(\dot{u}_{i,1}(t) + \frac{1}{2}b\,\dot{\theta}_i(t) - \dot{u}_{i,2L}\right)$$

$$\begin{aligned} Q_{i,1L}(t) = k_1\left(y_{2N+12i-11} + \frac{1}{2}b\,y_{2N+12i-9} - y_{2N+12i-7}\right) \\ + c_1\left(y_{2N+12i-10} + \frac{1}{2}b\,y_{2N+12i-8} - y_{2N+12i-6}\right) \end{aligned} \tag{B.23}$$

$$Q_{i,1R}(t) = k_1\left(u_{i,1}(t) - \frac{1}{2}b\,\theta_i(t) - u_{i,2R}\right) + c_1\left(\dot{u}_{i,1}(t) - \frac{1}{2}b\,\dot{\theta}_i(t) - \dot{u}_{i,2R}\right)$$

$$\begin{aligned} Q_{i,1R}(t) = k_1\left(y_{2N+12i-11} - \frac{1}{2}b\,y_{2N+12i-9} - y_{2N+12i-5}\right) \\ + c_1\left(y_{2N+12i-10} - \frac{1}{2}b\,y_{2N+12i-8} - y_{2N+12i-4}\right) \end{aligned} \tag{B.24}$$

$$\begin{aligned} Q_{i,2L} &= k_2\left(u_{i,2L} - u_{i,3L}\right) + c_2\left(\dot{u}_{i,2L} - \dot{u}_{i,3L}\right) \\ Q_{i,2L} &= k_2(y_{2N+12i-7} - y_{2N+12i-3}) + c_2(y_{2N+12i-6} - y_{2N+12i-2}) \end{aligned} \tag{B.25}$$

$$\begin{aligned} Q_{i,2R} &= k_2\left(u_{i,2R} - u_{i,3R}\right) + c_2\left(\dot{u}_{i,2R} - \dot{u}_{i,3R}\right) \\ Q_{i,2R} &= k_2(y_{2N+12i-5} - y_{2N+12i-1}) + c_2(y_{2N+12i-4} - y_{2N+12i}) \end{aligned} \tag{B.26}$$

$$\begin{aligned} Q_{i,3L} &= k_3\left(u_{i,3L}(t) - \sum_{n=1}^{N} w_{tn}(t)\,w_{xn}(vt_i - b)\right) \\ &\cdot H\left(u_{i,3L}(t) - \sum_{n=1}^{N} w_{tn}(t)\,w_{xn}(vt_i - b)\right) \\ Q_{i,3L} &= k_3\left(y_{2N+12i-3} - \sum_{n=1}^{N} y_{2n-1}\,\sin\left(\beta_n\,(vt_i - b)\right)\right) \\ &\cdot H\left(y_{2N+12i-3} - \sum_{n=1}^{N} y_{2n-1}\,\sin\left(\beta_n\,(vt_i - b)\right)\right) \end{aligned} \tag{B.27}$$

$$\begin{aligned} Q_{i,3R} &= k_3\left(u_{i,3R}(t) - \sum_{n=1}^{N} w_{tn}(t)\,w_{xn}(vt_i)\right) \cdot H\left(u_{i,3R}(t) - \sum_{n=1}^{N} w_{tn}(t)\,w_{xn}(vt_i)\right) \\ Q_{i,3R} &= k_3\left(y_{2N+12i-1} - \sum_{n=1}^{N} y_{2n-1}\,\sin\left(\beta_n\,(vt_i - b)\right)\right) \\ &\cdot H\left(y_{2N+12i-1} - \sum_{n=1}^{N} y_{2n-1}\,\sin\left(\beta_n\,(vt_i)\right)\right) \end{aligned} \tag{B.28}$$

$$\dot{y}_{2n-1} = \dot{w}_{tn}(t)$$
$$\dot{y}_{2n-1} = y_{2n} \tag{B.29}$$

$$\ddot{w}_{tn}(t) + {\omega_n}^2\, w_{tn}(t) = \sum_i \Big(f_n(vt_i) \cdot Q_{i,3L}(t) + f_n(vt_i) \cdot Q_{i,3R}(t) \Big)$$
$$\dot{y}_{2n} = \sum_i \Big(f_n(vt - s_i - b) \cdot Q_{i,3L}(t) + f_n(vt - s_i) \cdot Q_{i,3R}(t) \Big) - {\omega_n}^2\, y_{2n-1} \tag{B.30}$$

$$\dot{y}_{2N+12i-11} = \dot{u}_i(t)$$
$$\dot{y}_{2N+12i-11} = y_{2N+12i} \tag{B.31}$$

$$m_1 \ddot{u}_{i,1}(t) = m_1 g - Q_{i,1L}(t) - Q_{i,1R}(t)$$
$$\dot{y}_{2N+12i-10} = -\frac{1}{m_1}\Big(Q_{i,1L}(t) + Q_{i,1R}(t) \Big) + g \tag{B.32}$$

$$\dot{y}_{2N+12i-9} = \dot{\theta}_i(t)$$
$$\dot{y}_{2N+12i-9} = y_{2N+12i-8} \tag{B.33}$$

$$J\ddot{\theta}_i(t) = \frac{b}{2}\Big(-Q_{i,1L}(t) + Q_{i,1R}(t) \Big)$$
$$\dot{y}_{2N+12i-8} = \frac{b}{2J}\Big(-Q_{i,1L}(t) + Q_{i,1R}(t) \Big) \tag{B.34}$$

$$\dot{y}_{2N+12i-7} = \dot{u}_{i,2L}(t)$$
$$\dot{y}_{2N+12i-7} = y_{2N+12i-6} \tag{B.35}$$

$$m_2 \ddot{u}_{i,2L} = m_2 g + Q_{i,1L} - Q_{i,2L}$$
$$\dot{y}_{2N+12i-6} = \frac{1}{m_2}\big(Q_{i,1L} - Q_{i,2L} \big) + g \tag{B.36}$$

$$\dot{y}_{2N+12i-5} = \dot{u}_{I,2R}(t)$$
$$\dot{y}_{2N+12i-5} = y_{2N+12i-4} \tag{B.37}$$

$$m_2 \ddot{u}_{i,2R} = m_2 g + Q_{i,1R} - Q_{i,2R}$$
$$\dot{y}_{2N+12i-4} = \frac{1}{m_2}\big(Q_{i,1R} - Q_{i,2R} \big) + g \tag{B.38}$$

$$\dot{y}_{2N+12i-3} = \dot{u}_{i,3L}(t)$$
$$\dot{y}_{2N+12i-3} = y_{2N+12i-2} \tag{B.39}$$

$$m_3 \ddot{u}_{i,3L} = m_3 g + Q_{i,2L} - Q_{i,3L}$$
$$\dot{y}_{2N+12i-2} = \frac{1}{m_3}\big(Q_{i,2L} - Q_{i,3L} \big) + g \tag{B.40}$$

$$\dot{y}_{2N+12i-1} = \dot{u}_{i,3R}(t)$$
$$\dot{y}_{2N+12i-1} = y_{2N+12i} \tag{B.41}$$

$$m_3 \ddot{u}_{i,3R} = m_3 g + Q_{i,2R} - Q_{i,3R}$$
$$\dot{y}_{2N+12i} = \frac{1}{m_3}\big(Q_{i,2R} - Q_{i,3R} \big) + g \tag{B.42}$$

$$
\begin{gathered}
w_{tn}(0) = y_{2n-1,0} = 0 \\
\dot{w}_{tn}(0) = y_{2n,0} = 0 \\
u_{i,1}(0) = y_{2N+12i-11,0} = \left(\frac{m_1 + 2m_2 + 2m_3}{2k_3} + \frac{m_1 + 2m_2}{2k_2} + \frac{m_1}{2k_1}\right) g \\
\dot{u}_{i,1}(0) = y_{2N+12i-10,0} = 0 \\
\theta_i(0) = y_{2N+12i-9,0} = 0 \\
\dot{\theta}_i(0) = y_{2N+12i-8,0} = 0
\end{gathered}
$$

$$
\begin{gathered}
u_{i,2L}(0) = y_{2N+12i-7,0} = \left(\frac{m_1 + 2m_2 + 2m_3}{2k_3} + \frac{m_1 + 2m_2}{2k_2}\right) g \\
\dot{u}_{i,2L}(0) = y_{2N+12i-6,0} = 0 \\
u_{i,2R}(0) = y_{2N+12i-5,0} = \left(\frac{m_1 + 2m_2 + 2m_3}{2k_3} + \frac{m_1 + 2m_2}{2k_2}\right) g \\
\dot{u}_{i,2R}(0) = y_{2N+12i-4,0} = 0
\end{gathered}
\tag{B.43}
$$

$$
\begin{gathered}
u_{i,3L}(0) = y_{2N+12i-3,0} = \frac{m_1 + 2m_2 + 2m_3}{2k_3} g \\
\dot{u}_{i,3L}(0) = y_{2N+12i-2,0} = 0
\end{gathered}
$$

$$
\begin{gathered}
u_{i,3R}(0) = y_{2N+12i-1,0} = \frac{m_1 + 2m_2 + 2m_3}{2k_3} g \\
\dot{u}_{i,3R}(0) = y_{2N+12i,0} = 0
\end{gathered}
$$

Appendix C: Python code

Import packages

```
from numpy import *
from scipy.integrate import *
from scipy.interpolate import UnivariateSpline
from matplotlib.pyplot import *
%matplotlib inline
from mpl_toolkits.mplot3d import Axes3D
from datetime import *
```

General values

```
g   =    9.810     # m/s**2

# Bridge 1
l   =    6.000     # m
EI  =    3.332e9   # Nm**2
ρA  =    8.830e3   # kg/m
C   =    2.480e-2  # -
# Bridge 2
l   =   12.000     # m
EI  =   12.546e9   # Nm**2
ρA  =   12.300e3   # kg/m
C   =    2.060e-2  # -
# Bridge 3
l   =   24.000     # m
EI  =   53.380e9   # Nm**2
ρA  =   19.300e3   # kg/m
C   =    1.500e-2  # -
# Bridge 4
l   =   36.000     # m
EI  =  172.200e9   # Nm**2
ρA  =   17.000e3   # kg/m
C   =    0.500e-2  # -

# Vehicle
v   =   50.000     # m/s
b   =   17.400     # m
wagon=24.900       # m
m1  =   15.600e3   # kg
m2  =    3.200e3   # kg
m3  =    6.000e3   # kg
k1  =    1.200e6   # N/m
k2  =    4.400e6   # N/m
k3  =    1.270e9   # N/m
c1  =   34.440e3   # Ns/m
c2  =   52.210e3   # Ns/m

π=pi
ρAl=ρA*l
s=array([0*wagon,0*wagon+b,1*wagon,1*wagon+b,2*wagon,2*wagon+b,3*wagon,
3*wagon+b,4*wagon,4*wagon+b,5*wagon,5*wagon+b,6*wagon,6*wagon+b,7*wagon
,7*wagon+b])
p=500
n_max=10
t=linspace(0,(l+s.max())/v,p)
x=linspace(0,l,p)
```

General functions

```
def ß(n):
    return n*π/l
def ß2(n):
    return (n*π/l)**2
def ω(n):
    return(EI/ρA)**0.5*(n*π/l)**2
def ω2(n):
    return(EI/ρA)*(n*π/l)**4

def H(x):
    return heaviside(x,1)

def solve(model,tol=1.49012e-8):
    t1=datetime.now()
    wt=odeint(model,y0,t,rtol=tol,atol=tol)
    w=zeros((p,p))
    for n in arange(1,n_max+1):
        for i in range(p):
            for j in range(p):
                w[i,j]=w[i,j]+sin(ß(n)*x[i])*wt[j,2*n-2]
    t2=datetime.now()
    print('Δt =',t2-t1)
    print()
    print('w max =',round(1000*w.max(),9),'mm')

    M=0
    for j in range(p):
        y_spl=UnivariateSpline(x,w[:,j],s=0,k=4)
        x_range=linspace(x[0],x[-1],p)
        y_spl_2d=y_spl.derivative(n=2)
        if y_spl_2d(x_range).min()<M: M=y_spl_2d(x_range).min()
    M=M*-EI
    print('M max =',round(M/10**6,9),'kNm')
    u=np.zeros(p)

    if len(y0)==2*n_max+2*len(s):
        u=zeros((p,len(s)))
        for i in range(len(s)):
            u[:,i]=wt[:,2*n_max+2*i]-wt[0,2*n_max]
        print('u max =',round(1000*u.max(),9),'mm')

    elif len(y0)==2*n_max+4*len(s):
        u=zeros((p,2*len(s)))
        for i in range(len(s)):
            u[:,2*i+1]=wt[:,2*n_max+4*i]-wt[0,2*n_max+4*i]+1/2*b*wt[:,2
*n_max+4*i+2]
            u[:,2*i]=wt[:,2*n_max+4*i]-wt[0,2*n_max+4*i]-1/2*b*wt[:,2*n
_max+4*i+2]
        print('u max =',round(1000*u.max(),9),'mm')

    elif len(y0)==2*n_max+12*len(s):
        u=zeros((p,2*len(s)))
        for i in range(len(s)):
            u[:,2*i+1]=wt[:,2*n_max+12*i]-wt[0,2*n_max+12*i]+1/2*b*wt[:
,2*n_max+12*i+2]
            u[:,2*i]=wt[:,2*n_max+12*i]-wt[0,2*n_max+12*i]-1/2*b*wt[:,2
*n_max+12*i+2]
```

```
            print('u max =',round(1000*u.max(),9),'mm')

        if u.max()>0:
            a=0
            for i in range(len(u[0])):
                y_spl=UnivariateSpline(t,u[:,i],s=0,k=4)
                t_range=linspace(t[0],t[-1],1000)
                y_spl_2d=y_spl.derivative(n=2)
                aabs=abs(y_spl_2d(t_range))
                if a<aabs.max():a=aabs.max()

            print('a max =',round(1000*a,9),'mm/s2')

        return w,u,wt

def plotbeamovertime(t,w,X=l/2):
    figure(figsize=(16,9))
    plot(t,w[int(p*X/l)-1]*1000,linewidth=2)
    if X==l/2:title('Deflection at the middle of the beam',fontsize=22)
    else:title('Deflection at x = '+str(round(X,1))+str(' m'),fontsize=
22)
    xlabel('t (s)',fontsize=20)
    ylabel('w (mm)',fontsize=20)
    tick_params(labelsize=15)
    gca().invert_yaxis()
    grid(True);

def plotbeam2D(x,w,T=l/v):
    figure(figsize=(16,9))
    plot(x,w[:,int(p/2-1)]*1000,linewidth=2)
    title('Deflection at t = '+str(round(T,2))+str(' s'),fontsize=22)
    xlabel('t (s)',fontsize=20)
    ylabel('w (mm)',fontsize=20)
    tick_params(labelsize=15)
    gca().invert_yaxis()
    grid(True);

def plotbeam3D(x,t,w,count=100):
    T,X=meshgrid(t,x)
    fig=figure(figsize=(25,20))
    ax=fig.add_subplot(111,projection='3d')
    Axes3D.plot_surface(ax,T,X,1000*w,rcount=p,ccount=count,cmap=cm.hsv
,antialiased=False)
    ax.set_xlabel('t (s)',fontsize=30,fontstyle='oblique',labelpad=20)
    ax.set_ylabel('x (m)',fontsize=30,fontstyle='oblique',labelpad=20)
    ax.set_zlabel('w (mm)',fontsize=30,fontstyle='oblique',labelpad=20)
    for x in ax.xaxis.get_major_ticks():x.label.set_fontsize(30)
    for y in ax.yaxis.get_major_ticks():y.label.set_fontsize(30)
    for z in ax.zaxis.get_major_ticks():z.label.set_fontsize(30)
    ax.xaxis.pane.fill=False
    ax.yaxis.pane.fill=False
    ax.zaxis.pane.fill=False
    title('Deflection of the beam',fontsize=30)
    ax.invert_zaxis();

def plotvehicle(t,u):
    figure(figsize=(16,9));
    title('Deflection of the vehicle',fontsize=22);
```

```
    xlabel('t (s)',fontsize=20);
    ylabel('u (mm)',fontsize=20);
    tick_params(labelsize=20);
    gca().invert_yaxis();
    grid(True)
    plot(t,1000*u,linewidth=2)
    leg=[]
    if len(u[0])==len(s):
        for i in range(len(u[0])):
            leg.append('s = '+str(round(s[i],1))+str(' m'))
    elif len(u[0])==2*len(s):
        if len(s)==1:
            leg.append('front wheel')
            leg.append('rear wheel')
        else:
            for i in range(len(s)):
                leg.append('wagon '+str(i+1)+str(', front wheel'))
                leg.append('wagon '+str(i+1)+str(', rear wheel'))
    legend(leg,fontsize=20,loc='lower right',shadow=True,facecolor='whi
te');

def flyingwheel(wt):
    figure(figsize=(16,9));
    title('Deflection of the front wheel after passing the bridge',font
size=22);
    xlabel('t (s)',fontsize=20);
    ylabel('u (µm)',fontsize=20);
    tick_params(labelsize=20);
    gca().invert_yaxis();
    grid(True)
    u=wt[:,2*n_max+10]-wt[0,2*n_max+10]
    plot(t[t>l/v],10**6*(u[t>l/v]));

def compare(x,w,wref,Title='Comparison',Ylabel='Sum of errors over time
'):
    dwx=zeros(p)
    wgx=zeros(p)
    dw=abs(w-wref)
    for j in range(p):
        dwx[j]=sum(dw[j,:])
        wgx[j]=sum(abs(wG[j,:]))
    fig,ax=subplots(figsize=(16,9))
    ax.yaxis.offsetText.set_fontsize(15)
    plot(x[1:-1],dwx[1:-1]/wgx[1:-1],linewidth=2)
    title(Title,fontsize=22)
    xlabel('x (m)',fontsize=20)
    ylabel(Ylabel,fontsize=20)
    tick_params(labelsize=15)
    ticklabel_format(style='sci', axis='y', scilimits=(0,0))
    xlim(0)
    ylim(0)
    grid(True);
    print('Sum of all errors:', sum(dwx[1:-1]/wgx[1:-1]))
```

Solution of Graff

```
m=m1/2+m2+m3
Q=m*g

def Graff():
    t1=datetime.now()
    w=zeros((p,p))

    for n in range(1,n_max+1):
        for i in range(p):
            for j in range(p):
                w[i,j]=w[i,j]+sin(ß(n)*x[i])/(ω(n)*(ß2(n)*v**2-ω2(n)))*
(ß(n)*v*sin(ω(n)*t[j])-ω(n)*sin(ß(n)*v*t[j]))

    w=w*2*Q/ρAl
    t2=datetime.now()
    print('Δt =',t2-t1)
    print()
    print('w max =',round(1000*w.max(),9),'mm')

    M=0
    for j in range(p):
        y_spl=UnivariateSpline(x,w[:,j],s=0,k=4)
        x_range=linspace(x[0],x[-1],p)
        y_spl_2d=y_spl.derivative(n=2)
        if y_spl_2d(x_range).min()<M: M=y_spl_2d(x_range).min()
    M=M*-EI
    print('M max =',round(M/10**6,9),'kNm')

    return w

w=Graff()
```

Moving point load model

```
s=array([0,b])
y0=np.zeros(n_max*2)
m=m1/2+m2+m3

def model0(y,t):

    def f(n,t,i,b=0):
        return 2/ρAl*sin(ß(n)*(v*t-s[i]-b))*H(v*t-s[i]-b)*H(l-v*t+s[i]+
b)
    def Q(t,i):
        return m*g
    def fQ(n,t):
        result=zeros(len(s))
        for i in range(len(s)):
            result[i]=f(n,t,i)*Q(t,i)
        return result.sum()

    ydot=np.zeros(len(y))
    for n in arange(1,n_max+1):
        ydot[2*n-2]=y[2*n-1]
        ydot[2*n-1]=fQ(n,t)-ω2(n)*y[2*n-2]-2*C*ω(n)*y[2*n-1]*0
    return ydot

w,u,wt=solve(model0)
```

Moving oscillator

```
s=array([0,b])

m=m1/2+m2+m3
k=(1/k1+1/4/k2+1/4/k3)**-1
c=(1/c1+1/4/c2)**-1

y0=np.zeros(2*n_max+2*len(s))
for i in range(len(s)):
    y0[2*n_max+2*i]=m*g/k

def model1(y,t):

    def wtwx(t,s=0):
        wtwx=zeros(n_max)
        for n in arange(1,n_max+1):
            wtwx[n-1]=y[2*n-2]*sin(ß(n)*(v*t-s))*H(v*t-s)*H(l-v*t+s)
        return wtwx.sum()

    def wtdotwx(t,s=0):
        wtdotwx=zeros(n_max)
        for n in arange(1,n_max+1):
            wtdotwx[n-1]=y[2*n-1]*sin(ß(n)*(v*t-s))*H(v*t-s)*H(l-v*t+s)
        return wtdotwx.sum()

    def f(n,t,i,b=0):
        return 2/ρAl*sin(ß(n)*(v*t-s[i]-b))*H(v*t-s[i]-b)*H(l-v*t+s[i]+
b)

    def Q(t,i):
        return k*(y[2*n_max+2*i]-wtwx(t,s[i]))+c*(y[2*n_max+2*i+1]-wtdo
twx(t,s[i]))

    def fQ(n,t):
        result=zeros(len(s))
        for i in range(len(s)):
            result[i]=f(n,t,i)*Q(t,i)
        return result.sum()

    ydot=zeros(len(y))
    for n in arange(1,n_max+1):
        ydot[2*n-2]=y[2*n-1]
        ydot[2*n-1]=fQ(n,t)-ω2(n)*y[2*n-2]-2*C*ω(n)*y[2*n-1]
    for i in range(len(s)):
        ydot[2*n_max+2*i]=y[2*n_max+2*i+1]
        ydot[2*n_max+2*i+1]=-1/m*Q(t,i)+g
    return ydot

w,u,wt=solve(model1)
```

Moving oscillator with rotational inertia

```
s=array([0])

m=m1+2*m2+2*m3
J=1/12*m1*wagon**2+(m2+m3)*b**2/2
k=(1/k1+1/4/k2+1/4/k3)**-1
c=(1/c1+1/4/c2)**-1

y0=np.zeros(2*n_max+4*len(s))
for i in range(len(s)):
    y0[2*n_max+4*i]=1/2*m*g/k

def model2(y,t):

    def wtwx(t,s=0):
        wtwx=zeros(n_max)
        for n in arange(1,n_max+1):
            wtwx[n-1]=y[2*n-2]*sin(ß(n)*(v*t-s))*H(v*t-s)*H(l-v*t+s)
        return wtwx.sum()

    def wtdotwx(t,s=0):
        wtdotwx=zeros(n_max)
        for n in arange(1,n_max+1):
            wtdotwx[n-1]=y[2*n-1]*sin(ß(n)*(v*t-s))*H(v*t-s)*H(l-v*t+s)
        return wtdotwx.sum()

    def QL(t,i):
        return k*(y[2*n_max+4*i]+1/2*b*y[2*n_max+4*i+2]-wtwx(t,s[i]+b))
+c*(y[2*n_max+4*i+1]+1/2*b*y[2*n_max+4*i+3]-wtdotwx(t,s[i]+b))

    def QR(t,i):
        return k*(y[2*n_max+4*i]-1/2*b*y[2*n_max+4*i+2]-wtwx(t,s[i]))+c
*(y[2*n_max+4*i+1]-1/2*b*y[2*n_max+4*i+3]-wtdotwx(t,s[i]))

    def f(n,t,i,b=0):
        return 2/ρAl*sin(ß(n)*(v*t-s[i]-b))*H(v*t-s[i]-b)*H(l-v*t+s[i]+
b)

    def fQ(n,t):
        result=zeros(len(s))
        for i in range(len(s)):
            result[i]=f(n,t,i,b)*QL(t,i)+f(n,t,i)*QR(t,i)
        return result.sum()

    ydot=zeros(len(y))
    for n in arange(1,n_max+1):
        ydot[2*n-2]=y[2*n-1]
        ydot[2*n-1]=fQ(n,t)-ω2(n)*y[2*n-2]-2*C*ω(n)*y[2*n-1]
    for i in range(len(s)):
        ydot[2*n_max+4*i]=y[2*n_max+4*i+1]
        ydot[2*n_max+4*i+1]=-1/m*(QL(t,i)+QR(t,i))+g
        ydot[2*n_max+4*i+2]=y[2*n_max+4*i+3]
        ydot[2*n_max+4*i+3]=b/2/J*(-QL(t,i)+QR(t,i))
    return ydot

w,u,wt=solve(model2)
```

Moving oscillator with six degrees of freedom

```
s=array([0])
J=1/12*m1*wagon**2
y0=np.zeros(2*n_max+12*len(s))
for i in range(len(s)):
    y0[2*n_max+12*i]=(m1/2+m2+m3)/k3*g+(m1/2+m2)/k2*g+m1/2/k1*g
    y0[2*n_max+12*i+4]=(m1/2+m2+m3)/k3*g+(m1/2+m2)/k2*g
    y0[2*n_max+12*i+6]=(m1/2+m2+m3)/k3*g+(m1/2+m2)/k2*g
    y0[2*n_max+12*i+8]=(m1/2+m2+m3)/k3*g
    y0[2*n_max+12*i+10]=(m1/2+m2+m3)/k3*g

def model6(y,t):
    def wtwx(t,s=0):
        wtwx=zeros(n_max)
        for n in arange(1,n_max+1):
            wtwx[n-1]=y[2*n-2]*sin(ß(n)*(v*t-s))*H(v*t-s)*H(l-v*t+s)
        return wtwx.sum()
    def Q1L(t,i):return k1*(y[2*n_max+12*i]+1/2*b*y[2*n_max+12*i+2]-y[2
*n_max+12*i+4])+c1*(y[2*n_max+12*i+1]+1/2*b*y[2*n_max+12*i+3]-y[2*n_max
+12*i+5])
    def Q1R(t,i):return k1*(y[2*n_max+12*i]-1/2*b*y[2*n_max+12*i+2]-y[2
*n_max+12*i+6])+c1*(y[2*n_max+12*i+1]-1/2*b*y[2*n_max+12*i+3]-y[2*n_max
+12*i+7])
    def Q2L(t,i):return k2*(y[2*n_max+12*i+4]-y[2*n_max+12*i+8])+c2*(y[
2*n_max+12*i+5]-y[2*n_max+12*i+9])
    def Q2R(t,i):return k2*(y[2*n_max+12*i+6]-y[2*n_max+12*i+10])+c2*(y
[2*n_max+12*i+7]-y[2*n_max+12*i+11])
    def Q3L(t,i):return k3*(y[2*n_max+12*i+8]-wtwx(t,s[i]+b))*H(y[2*n_m
ax+12*i+8]-wtwx(t,s[i]+b))
    def Q3R(t,i):return k3*(y[2*n_max+12*i+10]-wtwx(t,s[i]))*H(y[2*n_ma
x+12*i+10]-wtwx(t,s[i]))
    def f(n,t,i,b=0):return 2/ρAl*sin(ß(n)*(v*t-s[i]-b))*H(v*t-s[i]-b)*
H(l-v*t+s[i]+b)
    def fQ3(n,t):
        result=zeros(len(s))
        for i in range(len(s)):
            result[i]=f(n,t,i,b)*Q3L(t,i)+f(n,t,i)*Q3R(t,i)
        return result.sum()
    ydot=zeros(len(y))
    for n in arange(1,n_max+1):
        ydot[2*n-2]=y[2*n-1]
        ydot[2*n-1]=fQ3(n,t)-ω2(n)*y[2*n-2]-2*C*ω(n)*y[2*n-1]
    for i in range(len(s)):
        ydot[2*n_max+12*i]=y[2*n_max+12*i+1]
        ydot[2*n_max+12*i+1]=1/m1*(-Q1L(t,i)-Q1R(t,i))+g
        ydot[2*n_max+12*i+2]=y[2*n_max+12*i+3]
        ydot[2*n_max+12*i+3]=b/2/J*(-Q1L(t,i)+Q1R(t,i))
        ydot[2*n_max+12*i+4]=y[2*n_max+12*i+5]
        ydot[2*n_max+12*i+5]=1/m2*(Q1L(t,i)-Q2L(t,i))+g
        ydot[2*n_max+12*i+6]=y[2*n_max+12*i+7]
        ydot[2*n_max+12*i+7]=1/m2*(Q1R(t,i)-Q2R(t,i))+g
        ydot[2*n_max+12*i+8]=y[2*n_max+12*i+9]
        ydot[2*n_max+12*i+9]=1/m3*(Q2L(t,i)-Q3L(t,i))+g
        ydot[2*n_max+12*i+10]=y[2*n_max+12*i+11]
        ydot[2*n_max+12*i+11]=1/m3*(Q2R(t,i)-Q3R(t,i))+g
    return ydot

w,u,wt=solve(model6)
```